Journal of
Marine Science and Engineering

MDPI

Review

A Review of Recent Developments in Friction Stir Welding for Various Industrial Applications

Shalok Bharti [1], Sudhir Kumar [2,*], Inderjeet Singh [1], Dinesh Kumar [2], Swapnil Sureshchandra Bhurat [2], Mohamed Ruslan Abdullah [3] and Seyed Saeid Rahimian Koloor [4,*]

1 Department of Mechanical Engineering, CT University, Firozpur Road, Ludhiana 142024, Punjab, India; shalokbharti8@gmail.com (S.B.); inderjeetsingh.pau@gmail.com (I.S.)
2 School of Engineering, DY Patil International University, Pune 411044, Maharashtra, India; dineshkumar.ap.19@gmail.com (D.K.); swapnilsbhurat@gmail.com (S.S.B.)
3 School of Mechanical Engineering, Universiti Teknologi Malaysia, Johor Bahru 81310, Malaysia
4 Institute and Laboratory for Structural Engineering, Department of Civil Engineering and Environmental Sciences, Universität der Bundeswehr München, Werner-Heisenberg-Weg 39, Neubiberg, 85579 Munich, Germany
* Correspondence: sudhirdwivedi1992@gmail.com (S.K.); seyed.rahimian@unibw.de (S.S.R.K.)

Abstract: Friction stir welding (FSW) has been recognized as a revolutionary welding process for marine applications, effectively tackling the distinctive problems posed by maritime settings. This review paper offers a comprehensive examination of the current advancements in FSW design, specifically within the marine industry. This paper provides an overview of the essential principles of FSW and its design, emphasizing its comparative advantages when compared with conventional welding techniques. The literature review reveals successful implementations in the field of shipbuilding and offshore constructions, highlighting design factors as notable enhancements in joint strength, resistance to corrosion, and fatigue performance. This study examines the progress made in the field of FSW equipment and procedures, with a specific focus on their application in naval construction. Additionally, it investigates the factors to be considered when selecting materials and ensuring their compatibility in this context. The analysis of microstructural and mechanical features of FSW joints is conducted, with a particular focus on examining the impact of welding settings. The study additionally explores techniques for mitigating corrosion and safeguarding surfaces in marine environments. The study also provides a forward-looking perspective by proposing potential areas of future research and highlighting the issues that may arise in the field of FSW for maritime engineering. The significance of incorporating environmental and economic considerations in the implementation of FSW for extensive marine projects is emphasized.

Keywords: design of marine structures; structural integrity; friction stir welding; welding technique; corrosion resistance

check for updates

Citation: Bharti, S.; Kumar, S.; Singh, I.; Kumar, D.; Bhurat, S.S.; Abdullah, M.R.; Rahimian Koloor, S.S. A Review of Recent Developments in Friction Stir Welding for Various Industrial Applications. *J. Mar. Sci. Eng.* **2024**, *12*, 71. https://doi.org/10.3390/jmse12010071

Academic Editors: Mahmoud Chizari, Okan Unal and Kazem Reza Kashyzadeh

Received: 23 November 2023
Revised: 16 December 2023
Accepted: 19 December 2023
Published: 27 December 2023

1. Introduction

In the current decade, the role of welding has become increasingly pivotal in meeting the demands of a rapidly advancing industrial landscape and diverse applications. As industries evolve to embrace innovative technologies and designs, welding serves as a fundamental process, addressing the intricate challenges posed by modern engineering. Welding encompasses various techniques, each tailored to specific applications and materials. Some prominent types include traditional methods such as arc welding (e.g., MIG, TIG, and stick welding) [1–3], oxy-acetylene welding [4], and more recent innovations such as laser welding [5]. Friction stir welding (FSW) has emerged as a cutting-edge alternative with distinct advantages over traditional welding methods [6].

Unlike traditional welding, which relies on melting and solidifying, FSW employs a solid-state process [7]. This characteristic minimizes the risk of thermal distortion, preserving the structural integrity of the materials being joined. Furthermore, FSW excels in welding dissimilar materials, a task that can be challenging for traditional methods due to differences in melting points and thermal expansion. FSW's solid-state nature allows it to seamlessly join materials with varying properties, opening doors to innovative applications in industries where dissimilar materials are prevalent [8,9].

FSW has gained significant recognition as a solid-state joining process across various industries since its inception in 1991 [10]. The fusion welding (FW) technique is gaining attention due to its ability to join alloys that are difficult to join using traditional methods. FSW offers several advantages over alternative welding processes, such as effectively joining materials that are not compatible with each other and reducing the cost of adhesives, self-piercing rivets, or other fasteners. Traditional welding procedures may negatively affect joint properties due to differing physical, chemical, and mechanical qualities. The FSW method is particularly suitable for linking materials that are not identical due to its significantly lower working temperature compared with the base material's melting point [11–13]. The use of this method, which offers numerous benefits such reduced costs, enhanced fatigue and tensile strength, a non-consumable tool, a low environmental impact, and increased sustainability, has significantly boosted the automotive manufacturing industry [14]. The process has gained significant importance in automotive manufacturing for its numerous benefits, including improved fatigue and tensile strength, non-consumption, eco-friendliness, and lower operating costs.

FSW is a rapidly developing welding technology with a wide range of potential applications in the marine industry [15]. Recent advancements in FSW have enhanced weld quality, efficiency, and productivity, making it more appealing for marine applications. New tool designs, such as those with multiple pins and shoulders, reduce welding forces and enhance weld strength [16]. Automated FSW systems enhance consistency and productivity in welding large, complex structures. Hybrid FSW processes, which combine FSW with other welding methods such as arc or laser welding, improve the weld quality and efficiency for specific applications [17,18]. FSW is utilized in various marine applications, including shipbuilding, ship repair, and offshore structures. It is used to weld aluminum alloy panels, deck panels, and repair the damaged components of ships. FSW is also used to weld aluminum alloy components in offshore structures such as oil platforms and wind turbines [19,20]. The FSW technique is widely used for welding materials with similar or dissimilar properties, particularly in the automotive sector due to its lower temperature level. It allows for various types of dissimilar joining for various combinations, such as Al/Mg (demonstrating its versatility in various applications [21]), Al/steel, and Al/Ti [22].

Methods that utilize machine learning (ML) have gathered significant attention as viable models for modeling a variety of manufacturing systems in recent years [16,23,24]. Machine learning applications have been seen in the FSW field as well. ML approaches have demonstrated interesting applications in a variety of engineering fields, including fracture mechanics [25], structural engineering [26], composite materials [27], laser cutting [28], measurement science [29], metal cutting [30], and friction stir processing [31] to name a few. Different FSW technologies have unique welding parameters and conditions, making modeling the process challenging and time intensive. Machine learning (ML) approaches are proposed for modeling FSW due to their ability to understand the relationship between control variables and welding process responses during training, as they can learn from mistakes [32].

The review paper explores the advancements in flexible welding (FSW) for marine applications, highlighting its advantages over conventional methods. It discusses improvements in joint strength, corrosion resistance, fatigue performance, FSW equipment, material selection, corrosion mitigation, surface protection, and machine learning approaches. It suggests future research and emphasizes the importance of considering environmental and economic factors in FSW implementation.

2. Fundamentals of Friction Stir Welding

FSW is an advanced solid-state welding technique that creates strong, high-quality joints between metals without melting them. It employs a specialized tool with a shoulder and a rotating pin [33,34]. As the tool is plunged into the joint, friction generates heat, softening the material without liquifying the material. This results in a plasticized zone where the material becomes adaptable, allowing for grain refinement and mixing [35]. The tool's rotation stirs and blends the material, forming a defect-free joint as it propagates along the weld line. FSW is particularly useful for joining materials such as aluminum and other non-ferrous alloys, providing superior strength and minimal distortion and making it valuable in the aerospace and automotive industries alongside many others [36–39]. Figure 1 shows a schematic diagram of the FSW process.

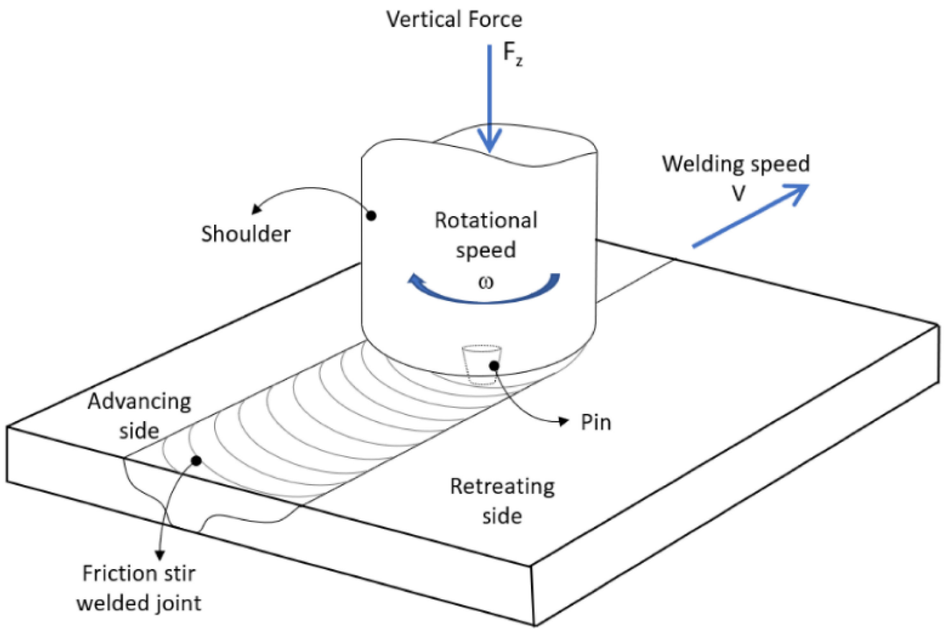

Figure 1. Schematic of the FSW process.

2.1. Tool Design and Material Flow in the FSW Process

The FSW tool consists of two main components, the shoulder and the pin; each is designed for specific welding processes. The shoulder, larger and flat, provides downward force for holding workpieces together, whereas the pin is suitable for thinner materials [40]. The shoulder is typically made from a wear- and heat-resistant material, such as tungsten carbide [41–43]. FSW tools often have cooling systems to dissipate the heat generated during welding, ensuring tool life and reducing the frictional forces and heat [44,45]. The pin is the smaller, threaded or profiled part of the tool that penetrates the joint. The size and profile of the pin are crucial for controlling material flow and ensuring the desired joint properties [46]. The pin, made from wear- and heat-resistant material, should be chosen based on the joint requirements and operating conditions. The pin rotates during welding, affecting the material flow and weld characteristics. Proper selection of profile, rotation direction, and speed is crucial for joint quality [47–49]. FSW tools with retractable pins control the penetration depth during welding and are useful for materials with varying thicknesses or joint control. Thread design affects material mixing and flow. Threaded pins [50] are often used to enhance material mixing and improve joint quality.

The FSW process significantly influences the quality and integrity of a weld by controlling the material flow within the plasticized zone, a region of the workpiece that becomes soft and pliable due to frictional heat generated by the rotating tool. This material flow can be described as shown in the Figure 2.

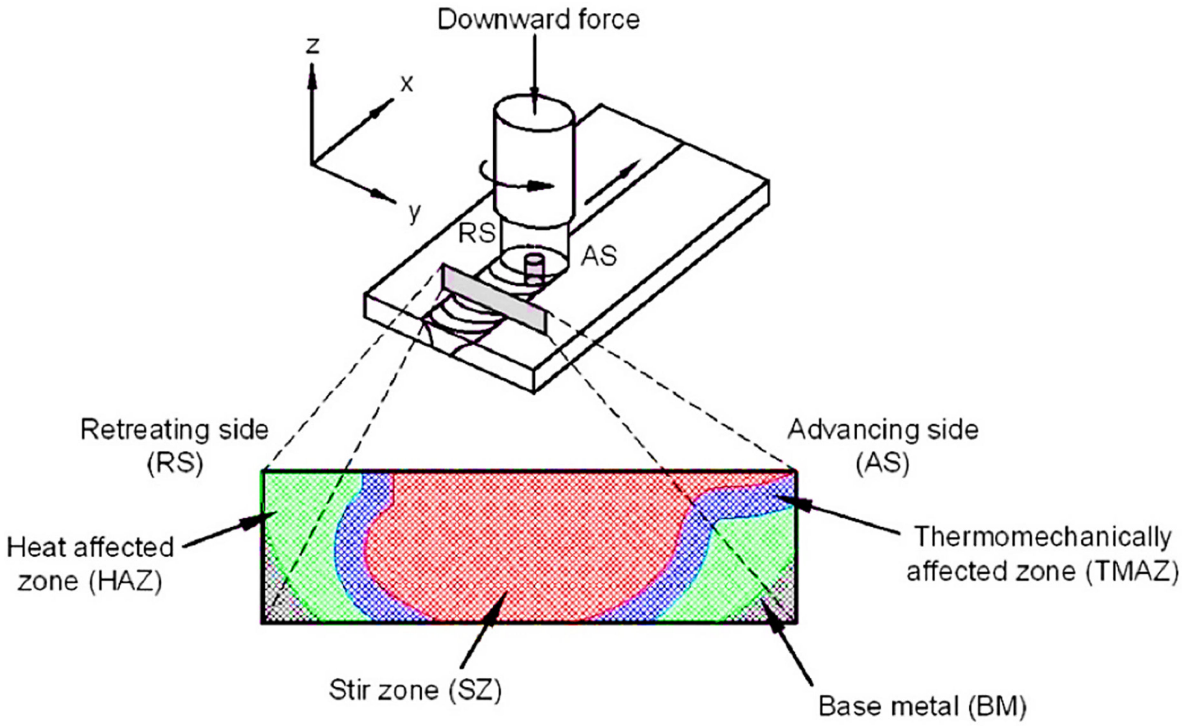

Figure 2. Different welding zones in the FSW process [51].

The rotating FSW tool generates frictional heat, softening material around it and creating a plasticized zone. This process breaks down grain structure, resulting in a finer weld zone and eliminating defects such as voids and inclusions, a common issue in traditional fusion welding. The FSW tool promotes metallurgical bonding, forming a strong, defect-free joint. As it progresses, the material solidifies forming the weld joint, with the "weld nugget" achieving highest strength [51].

2.2. FSW in Marine Applications

FSW is increasingly being used in marine applications due to its durability, corrosion resistance, and structural integrity, making it an attractive choice for welding and fabricating components such as hulls and bulkheads [52]. The FSW welding method extends the vessel and component lifespan in marine applications due to minimal heat input and low distortion, reducing intergranular and stress corrosion issues. This is advantageous in marine environments where there is exposure to saltwater and harsh weather conditions [53,54].

FSW is a solid-state welding process that generates significantly less heat compared with fusion welding methods such as arc welding. This results in the reduced distortion [55] and warping of components, ensuring tighter dimensional control and alignment, which is crucial in shipbuilding to maintain the integrity and hydrodynamics of the vessel. It also produces high-quality, defect-free welds with no solidification-related defects such as porosity or hot cracking [56]. Fusion welding (FSW) ensures structural integrity and minimizes post-weld inspections. It can join dissimilar materials such as aluminum to steel or copper alloys to aluminum, optimizing the weight, strength, and corrosion resistance in marine applications, unlike traditional methods [57–60].

2.3. Parameters Influencing the FSW Process

The FSW process is influenced by key parameters that determine the weld quality and efficiency. Optimizing these parameters for specific applications is crucial for producing high-quality, defect-free welds with the desired mechanical properties [61,62]. Adjusting these parameters allows for flexibility in FSW, making it a versatile technique for joining a wide range of materials and components.

The rotation speed of an FSW tool significantly impacts heat generation, material softening, and flow. Higher speeds can speed up welding but may increase tool wear and decrease material flow control. Traverse speed allows a thorough mixing and material flow but increases heat input and cycle time. Faster traverse speeds may reduce heat input but may also lower joint quality [63–65].

The materials from which the FSW tool is made can significantly impact the process. Tool materials must have high wear resistance and withstand the mechanical and thermal stresses of the welding. Common tool materials include tungsten carbide [41,44], tool steel [66], and cermet materials. The tool material choice should be compatible with the workpiece materials to prevent contamination and facilitate proper material flow.

The design of the FSW tool, including the pin and shoulder shape, impacts the material flow, heat generation, and joint quality. The pin profile and shoulder size are customized for specific applications. Tilt angles can optimize welding processes for different materials and joint configurations [67,68]. The applied downward force that is exerted by the FSW machine affects the material contact and friction between the tool and the workpieces. It must be carefully controlled to ensure proper material flow and joint quality [69]. The material used in welding significantly influences the FSW process, affecting tool parameters and requiring adjustments for thicker materials or complex geometries.

Some FSW setups incorporate cooling systems to regulate the temperature during welding. Proper cooling can help manage the heat generated and prevent material overheating or tool wear [70]. The welding environment, such as the presence or absence of inert gases [71] or shielding [72], can also affect the FSW process, particularly for materials prone to oxidation.

3. Friction Stir Welding for Marine Applications

FSW is a highly efficient marine welding method used for combining metals that produces superior-quality welds due to its reduced distortion, enhanced mechanical qualities, and increased corrosion resistance, making it preferred for ship construction [73]. Feistauer et al.'s study evaluated the mechanical properties of FSW on tailor-welded blanks (TWB) in the shipbuilding industry. They used a digital image correlation method to describe the joints made from different Al–Mg alloys. The joints showed superior performance compared with AA5059 base material and showed strength to 70 MPa [74]. Aluminum is commonly used in complex marine construction due to its high strength-to-weight ratio, low density, corrosion resistance, ease of fabrication, and recycling [75]. Researchers have optimized the friction stir welding of the aluminum plates AA5052-H32, achieving an efficiency of 93.51% at a 1.5° tilt angle, promising applications in shipbuilding [76]. The Taguchi method was used to optimize the performance of aluminum 5451 alloy structures in marine applications, achieving a maximum hardness of 81.056 HV and a tensile strength of 160.6907 MPa [14].

Figure 3 illustrates the use of friction stir welding (FSW) in marine applications, particularly in shipbuilding, where higher efficiency and corrosion resistance are required. Konkol PJ et al.'s study on FSW in shipbuilding demonstrated the techniques potential for ferrous alloy applications. They successfully achieved single-pass and two-pass weldments in HSLA-65 steel that demonstrated satisfactory properties such as transverse tensile strength, ductility, and corrosion resistance [77]. Corrosion significantly impacts structures and weakens joints during welding processes; however, FSW provides leakproof and corrosion-resistant welding joints. D.M. Sekban et al.'s study on the FSW of low-carbon steel plates in shipbuilding found improvements in microstructure, hardness, mechanical strength, ductility, formability, and corrosion resistance [78]. FSW is a popular method for subsea pipelines, providing a strong, seamless joint and reducing the need for traditional underwater welding techniques. It offers enhanced structural integrity (tensile strength: 218 MPa) and corrosion resistance (32 VHN), making it suitable for marine environments. A study comparing UWFSW and traditional FSW on AA 6063 pipes found UWFSW superior due to higher tensile strength, corrosion resistance, and durability [79]. UWFSW offers improved corrosion resistance and higher tensile strength and nugget-zone hardness, making it a promising technique for marine applications and enhancing the structural integrity and durability of welded pipes [79,80]. Underwater FSW (UWFSW) on an Al 6063 alloy demonstrated a high efficiency of 92.7% for ultimate tensile strength at a 4 rpm traverse speed and a 1800 rpm rotational speed, with excellent mechanical properties such as a fine grain structure and low porosity [81]. Friction stir welding (FSW) is a versatile welding method used in various sectors, including offshore structures for dependable connections and propellers for increased strength and durability, that ensures connections can withstand marine conditions [82]. A study on friction-stir-welded joints in DH36 steel revealed that marine-grade FSW outperformed fusion welds, suggesting the potential use of a recently developed S-N curve in fatigue assessment guidelines for low-alloy steel FSW [83].

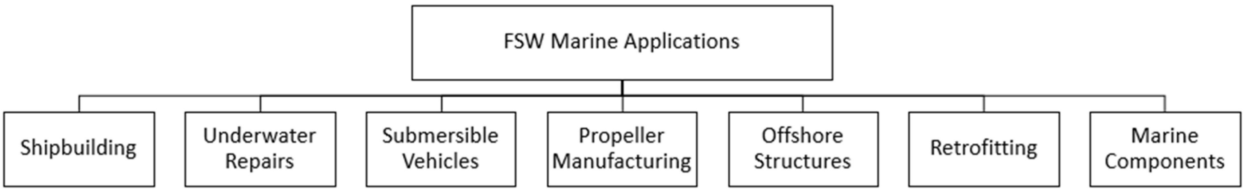

Figure 3. Application areas of FSW in marine engineering.

FSW is crucial for underwater maintenance and repairs of offshore infrastructure, including pipelines and oil rigs. It can also prevent corrosion-related damage and ensure structural integrity in difficult aquatic environments [84]. A study by Lader SK et al. found that the UWFSW of brass and aluminum alloy lap joints produced stronger joints, a better microstructure, and fewer welding faults, with tensile strength improvements of 42%, 30%, and 50% compared with C-FSW [85].

4. Recent Technological Advancements in Friction Stir Welding

The last decade has seen a rise in friction stir welding for marine applications. Several developments have been seen in terms of tooling and fixtures, the welding technique (especially in-service repair), material combination for high-strength alloys and dissimilar metals, the optimization of welding conditions, improved corrosion resistance, the use of AI and robotics in marine applications, etc., [86,87].

4.1. Developments in Friction Stir Welding Tools and their Design

The friction stir welding setup has evolved over the past five years, with studies comparing double shoulder with spiral pin and double spiral tools on the shoulder. The results showed that spiral pins on the shoulder degrade the weld quality and strength, leading to a poor joint and internal cracks [15]. A study on the impact of the tool plunging rate on the mechanical and surface properties of the DMR294A high-strength alloy found that an increased plunging rate had a negative effect on the mechanical properties [88].

The tool profile significantly influences the mechanical and morphological properties of friction-stir-welded alloys. A study found that the square pin profile was superior to other profiles tested for the AA6061-T6 alloy, indicating that the tool design significantly influences the surface profile and internal stress during FSW, making it a crucial variable in FSW [89]. A study developed a new static shoulder friction stir welding (SSFSW) tool to mitigate the grain coarsening caused by friction and excessive temperature. The tool, which included rotating and non-rotating shoulders, was tested under various friction stir welding conditions. The results showed that the tool reduced internal stresses, increased γ-fiber presence, and improved formability by 7.2% [90]. Figure 4 shows the developed novel tool that held many subparts, as depicted in the figure.

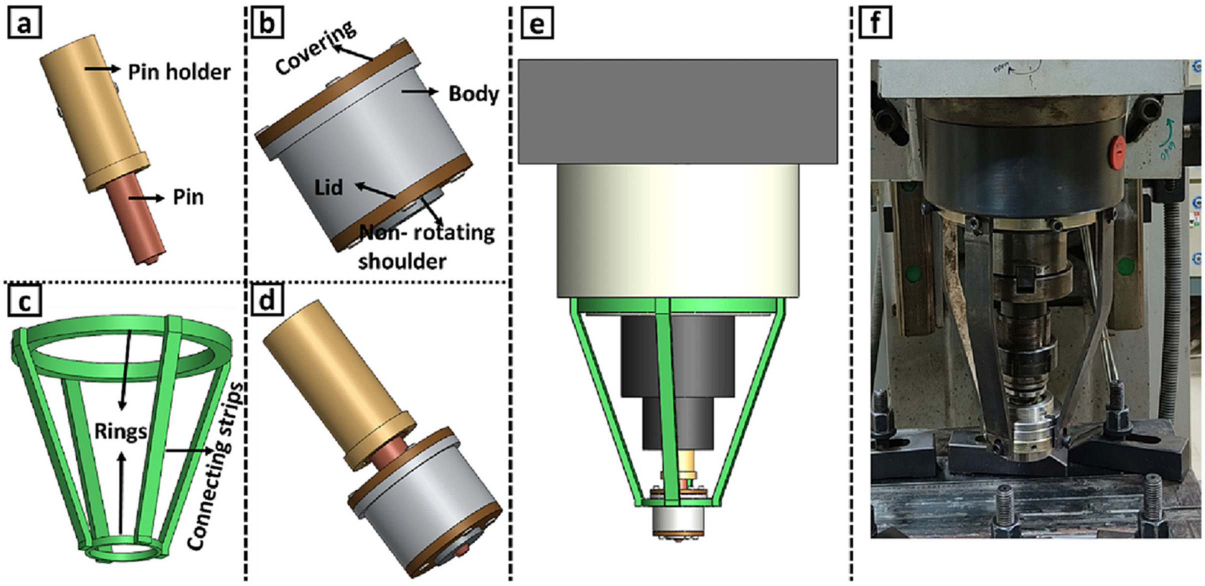

Figure 4. Developed novel SSFSW tool: (**a**) rotating pin, (**b**) non-rotating outer assembly, (**c**) connecting strip part, (**d**) assembly of the tool, (**e**) assembled tool with connecting strip, and (**f**) real-time tool on machine (reused with permission from Ref [90]).

A study analyzed the heat behavior near joints using numerical modeling for three types of tools: pinless, shoulderless, and complete tools with a shoulder and pin. Pinless tools produced lower temperatures, with almost 90% of the required temperature produced by the shoulder alone. The study found that the presence of both a shoulder and a pin in the tool caused strain in the heat zone, with lower strains observed for the pinless and shoulderless tools [91]. One of the studies suggested the use of a pneumatic-powered FSW tool. The study found that pneumatic-powered FSW tools could be used for polymeric welding, the repair of motorboats and car bumpers, and onsite repairs, etc., [92]. A study recommends using a thin-walled steel tool for FSW and working at different rotational speeds and contact times. A conical and slim tool geometry with small shoulders is recommended for the speedy penetration and deep plunging of workpieces [93]. Figure 5 shows the conical geometry of the FSW tool optimized for the better mechanical strength of joints. A study found that the shoulder area generally has lower temperature generation than the pin area, despite its dominant role in workpiece temperature generation [94]. A study linked the tool contact pressure to process void defects and observed a decrease in tool service life with increasing the tool rotational speed [95]. The study tested tool eccentricity and welding speed on three eccentric points (0, 0.2, and 0.8 mm) for constant rotation at 600 rpm and varying welding speed from 100 to 500 mm/min, determining maximum joint strength [96].

FSW is a process that affects the surface profile and internal stress created during the welding process. Spiral pins on the shoulder have been found in studies to reduce weld quality and strength, resulting in weak joints and interior cracks. The tool plunging rate also affects the mechanical and morphological properties of FSW alloys. According to one study, a square pin profile for the pin was superior to the other profiles studied. The surface profile and internal stress were also influenced by tool design. A new static shoulder friction stir welding (SSFSW) tool was developed in order to prevent the grain coarsening caused by friction and high temperatures. Heat generation and dissipation are influenced by the tool shoulder and pin. One study created a way for connecting HDPE and carbon black CB materials using the FSW process. The research team created a novel tool with a shoulder and a tool guide to construct flange-to-pipe couplings. Figure 6 depicts the designed tool, which is made from H13 steel. The newly invented too l was utilized to weld the tube to the rectangular sheet in order to create leakproof flange-to-pipe junctions [97].

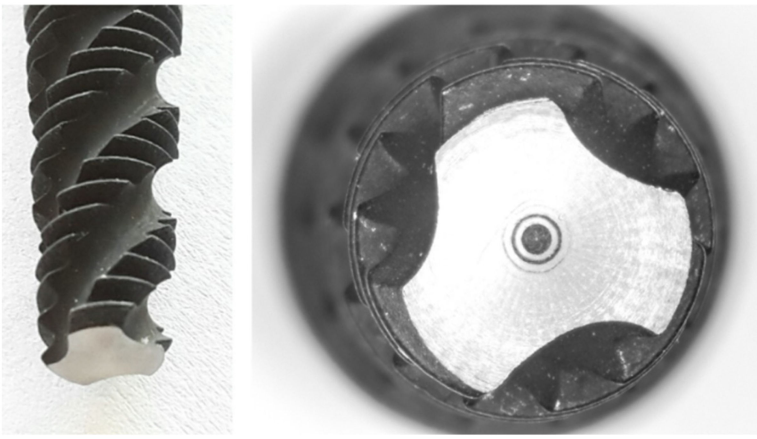

Figure 5. Optimized tool for speedy penetration and deep plunging (reused with permission from Hossfeld, Ref [93]).

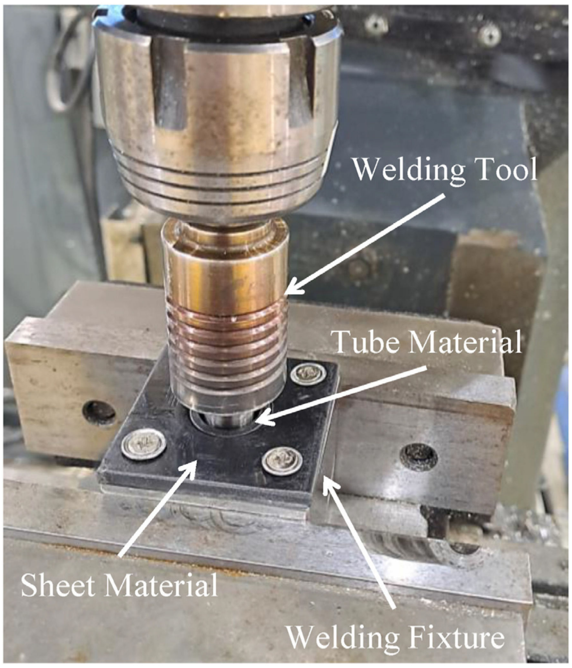

Figure 6. Newly designed tool to weld HDPE–CB material for flange-to-pipe joints (reused with permission from Ref [97] http://creativecommons.org/licenses/by-nc-nd/4.0/ accessed on 13 December 2023).

Researchers have investigated FSW utilizing a cryogenic setup in which −196 °C liquid nitrogen was employed to enhance the FSW process. The tensile and hardness parameters of the welded ZE42 magnesium alloy improved by 41% and 35%, respectively, according to the study. The study also discovered a reduction in sample wear properties when welded with a cryogenic FSW setup over the standard FSW technique. The FSW system was modified using a liquid nitrogen hose pipe delivered to the welding zone. Figure 7 shows a modified FSW setup for ZE42 magnesium alloy welding [98].

A similar type of study has a modified setup using a cooling media in circulation below the base plate to be welded. The study observed proper grain growth when welding with cooling media compared with normal FSW [99]. Figure 8 shows the designed setup with the cooling media attachment below the base plate. One study employed a pneumatic arrangement to rotate the tool for the FS welding of polymeric samples with an ABS-based consumable tool for polymeric sheets. The study modified a pneumatic machine holder to hold the tool, which was replaced by a chuck base arrangement [100].

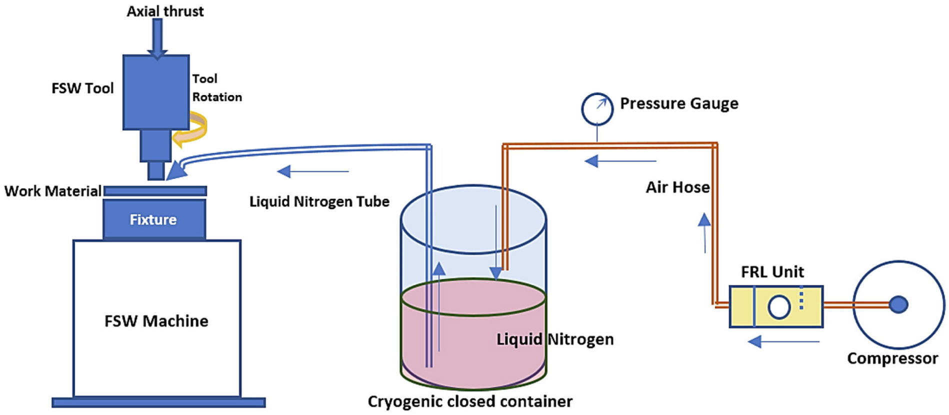

Figure 7. Modified setup of FSW with a cryogenic setup (reused with permission from Ref [98] http://creativecommons.org/licenses/by-nc-nd/4.0/accessed on 13 December 2023).

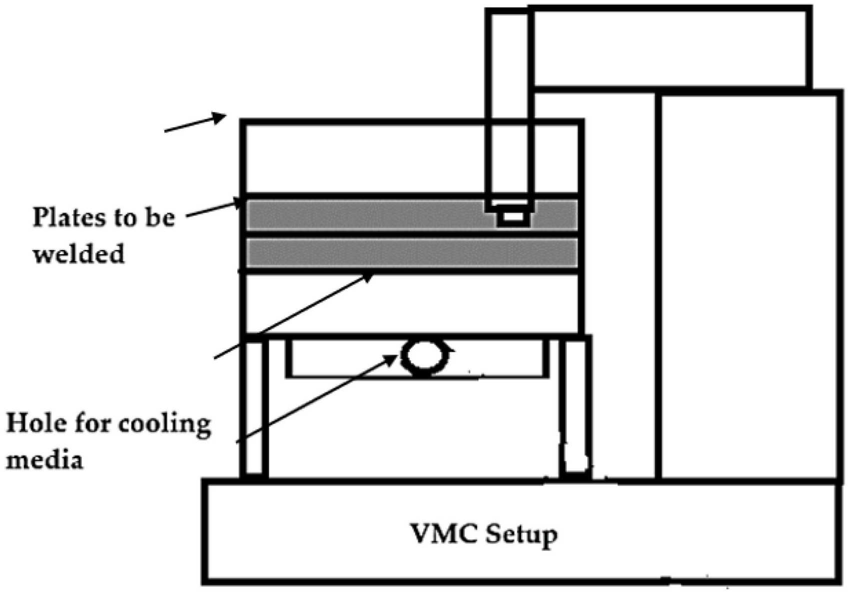

Figure 8. Schematic for the indirect cooling of the workpiece setup for FSW.

Senff and Volk [101] proposed a combination of compound casting and an FSW setup for the bimetal joining of aluminum and steel specimens. According to the findings of the study, if steel specimens are placed in the pressure die casting process and the resulting specimens are then subjected to the FSW technique at the boundary of the AL and steel material, the joining strength can be attained as required. Akbari and Asiabaraki [102] optimized the forces generated by the FSW setup using a newly designed fixture. The forces produced by the FSW setup when welding the specimen were proportional to the joint strength, welding circumstances, and tool shape.

4.2. Material Combination and Process Optimization Developments

FSW has been in high demand to weld various dissimilar materials. These various materials play an important role in industrial applications. The need for FSW, or the process of combining different materials, has increased noticeably over the last ten years. This is mostly due to the unique advantages that these materials offer, such as improved strength, higher corrosion resistance, and increased design freedom. It is expected that the importance of welding dissimilar materials using FSW will grow even more in the next few years as companies continue to investigate new applications and technological improvements [103].

Noga et al. [104] used electron beam welding as well as an FSW setup to connect an EN AW6082 T6 alloy. A rotational speed of 710 rpm and a welding speed of 355 mm/min were used for the FSW. The mechanical strength of the joints was lower than that of the parent metal. FSW had a higher peak elongation (7.2%) than an EBM-welded workpiece (2.7%), despite the fact that EBM-welded workpieces had higher mechanical strength and brittleness than FSW-welded samples [104]. Liu et al. [105] investigated the microstructural evolution of AA1050 Al alloy FSW. According to the study, the temperature profile of FSW becomes constant during the acceleration stage. Similarly, as minute changes in the range of crystal growth were observed, velocity grain recrystallization and plastic deformation reached a state of equilibrium. Grain coarsening began in the final step of low acceleration thermal activation [105].

Singh and Kumar [106] devised a revolutionary procedure in which they added a cooling tank to the bottom of the welding plates. The FSW bead was cooled using air, water, and cooling media in the study. The study discovered that the quenching of the parts and thinning of the weld part were the main challenges for the direct cooling of the workpiece, but the new configuration devised and used in the study alleviated the issue, allowing the FSW setup to maintain uniform heating and cooling. The highest strength for the ICFSW process was found to be 153.16 MPa at a 500 rpm tool rotation.

One of the research projects focused on the optimization of FSW working conditions for AA-7075-T651 Al alloys with a sheet thickness of 6 mm. For the FSW method, a non-consumable tool pin made from H13 tool material was used. The study determined that the best FSW working conditions were 800 rpm and a 50 mm/min feed rate. The weld zone material had a maximum strength of 278 MPa, which was 50% of the strength of the foundation material [107]. The effect of multi-pass roll and annealing on FSW samples of AZ31 alloy was studied by researchers. The study discovered that multi-pass hot rolling and annealing had a good effect on the mechanical qualities of the welded junction. The sample's ultimate strength increased from 308 MPa to 383 MPa, whereas the percentage elongation increased from 17.5 to 21.3 [108].

One study optimized the operating conditions of FSW for AA5052 thin plate. The study found a tool rotation of 350 rpm, 900 Kg of axial load, and 550 mm/min of welding speed as the standard optimum FSW running conditions [109]. A study performed by Kumar et al. [110] observed that when the traverse speed of welding was increased keeping the tool rotation constant, the process adversely affected the mechanical strength of the welded joint. Vallavi and Madhavan explored the FSW of dissimilar alloys of Al grade AA6082 and AA5052. The study observed that the pin profile had a significant impact on the mechanical characteristics of the prepared weld. A maximum strength of 185 MPa was observed for the square type of pin profile, which had the highest joint efficiency of 96.35% [111]. Laska and others performed an experimental investigation on the corrosion behavior of dissimilar material welds of AA6082 and AA6060 in the presence of NaCl ions as the Cl- ion initiates the corrosion of the material under seawater conditions. The study observed an increase in the grain length in comparison with the base metal in the weld zone with increased residual stresses. The higher linear feed rate of 200 mm/min resulted in low residual stresses [112].

One study looked at dissimilar FSW welds for AA6082 and AA5456 plates. The gray relational analysis technique was employed in the study to turn the multi-objective task into a single single-objective study. The study's findings indicate that the tool speed is the most important parameter in comparison with other variables such as traverse speed, tool profile, tilt angle, and so on. The study recommended improved FSW, running settings of 200 mm/min traverse speed, 1000 rpm tool rotation speed, 10 tool tilt angle, and a 4 mm depth of pin. The results also revealed that a straight pin with the optimal conditions outperformed the threaded and taper pin profiles [113]. Datta et al. compared submerged FSW with conventional FSW by increasing the welding speed from 30 to 60 mm/min at 15 min intervals while maintaining the tool rotation constant at 1200 rpm. In the case of conventional FSW, the results indicated that the maximum strength was observed with a maximum welding speed of 60 mm/min. In the instance of underwater FSW, a 45 mm/min traverse speed gave the samples the maximum mechanical strength [114].

Other authors explored dissimilar FSW for A6061 and AA7075 Al alloys and optimized the process parameters. The study suggested that a tool rotation of 1164 rpm, tool traverse speed of 32 mm/min, and a SiC particle in FSW weld zone of 8.7 percent by volume led to the maximum tensile strength of the joint of 252 MPa and a microhardness of 178HV [115]. Similarly, another study looked at how the plate position affected the FSW properties for AA6061 and AA6082. When AA6082 was placed on the advancing side of FSW, the mechanical strength increased. Along the weldment sample of AA3082-AA6061, a maximum tensile strength of 218 MPa was found [116]. A comparable study looked at the influence of placement on the mechanical properties of AA1050-H14 and AA6082-T6 Al alloys. The study discovered that when AA1050-H14 was positioned on the advancing side, the joint had higher mechanical strength under the same processing conditions as FSW (tool rotation of 1200 rpm, traverse speed of 40 mm/min, and tool tilt of 20) [117].

Wang and Xu investigated the effect of a unique heat treatment procedure on grain coarsening in an Al2219 alloy. The investigation used an intermediate heat treatment technique that involved heating and annealing the FSW workpieces. Following the solution treatment of the weld nugget, the study used heat treatment. The study discovered that this intermediate heat treatment technique improved the weld strength by 20%. Crack propagation along the grain boundary was discovered to decrease during the process [118]. Using the FSW technique, one study presented a novel strategy for welding tubular components. The researchers proposed a new tool design with a concave shoulder and angles of 30, 60, and 90. The 30° concave tool demonstrated the maximum strength with the fewest pores. Surface roughness was improved for greater angle concavities [119].

Jain and Mishra worked on joining AA6061 and AA7075 using the FSW technique and Al_2O_3 reinforcement as a particle in the weld zone. The study focused on the optimization of tool rotation speed, traverse speed, and Al_2O_3 volume percentage. The results of the study suggested a tool speed of 971 rpm, a traverse speed of 40 mm/min, and an Al_2O_3 vol percentage of 10% as the optimum processing conditions, with a maximum joint strength of 226.2 MPa and a microhardness of 144.3 HV [120]. One study evaluated the corrosion behavior of an FS-welded Al6061-T6/AZ31 dissimilar alloy by varying the pH values of the testing environment. Maximum corrosion was observed for sample A1 (a tool rotation of 560 rpm and a traverse speed of 16 mm/min), with the lowest pH value of 2. The study established that with increasing welding speed there was a decrease in the corrosion rate. Cryogenic Charpy testing at −40 °C for the samples showed that with a decrease in temperature, the sample held a lower impact strength that reduced by up to 57% for sample A2 (FS-welded with a speed of 20 mm/min) [121].

In one study, the authors evaluated the optimized conditions of formability for the FSW of dissimilar materials of AA6061 and AA2017 using simulation and the experimental environment. The study observed a tool rotation of 1300 rpm, a traverse speed of 20 mm/min, and a tool tilt angle of 1° were the optimized conditions for joining dissimilar materials through FSW in comparison with any other conditions tested in the study [122]. A similar study was performed on the evaluation of the curvature radius of the tool on weld performance. The study observed a curvature radius of less than 7 mm resulted in the accumulation of the welding material. A curvature radius of 7 mm was observed to be a critical value, as a decrease in this value resulted in poor joint performance and values above it resulted in better strength [123]. The researchers also evaluated the effect of pin eccentricity on weld joints for AA5754-H111 and AA6101-T6 alloys. The study observed that a 900 rpm tool rotational speed, a traverse speed of 40 mm/min, and a pin eccentricity of 0.35 mm were the optimized conditions for the FSW of the dissimilar alloys selected for the study [124].

Table 1 shows the summary of the studies performed under technological advancement in recent years for the optimization of the processing conditions of the FSW process.

Table 1. Summary table for the technological advancement of optimization work.

S. No.	Research Focus	Key Findings	Author and Reference
1	Joining EN AW6082 T6 alloy using EBM and FSW.	EBM resulted in high mechanical strength but brittle nature. FSW had better peak elongation.	[104]
2	Microstructural evolution of the FSW of AA1050 Al alloy.	The temperature profile stabilized during the acceleration stage. Balance stage for grain recrystallization and deformation.	[105]
3	Development of a novel FSW technique with cooling tank.	Novel setup improved uniform heating and cooling. Maximum strength was observed at 153.16 MPa for the ICFSW process.	[106]
4	Optimization of FSW conditions for AA-7075-T651 Al alloys.	Optimal conditions: 800 rpm tool rotation and 50 mm/min feed rate. Maximum strength of 278 MPa.	[107]
5	Effect of multi-pass rolling and annealing on FSW of AZ31 alloy.	Improved ultimate strength from 308 MPa to 383 MPa with increased elongation.	[108]
6	Optimization of FSW conditions for AA5052 thin plate.	Standard optimum conditions: 350 rpm rotation, 900 Kg axial load, and 550 mm/min welding speed.	[109]
7	Effect of increased traverse speed on the mechanical strength of FSW joints.	Increased traverse speed negatively affected mechanical strength.	[110]
8	FSW of dissimilar alloys (AA6082 and AA5052) with different pin profiles.	The square pin profile yielded maximum strength (185 MPa) with 96.35% joint efficiency.	[111]
9	Corrosion behavior of dissimilar material weld (AA6082 and AA6060).	Increased linear feed rate (200 mm/min) reduced residual stresses.	[112]
10	Evaluation of dissimilar FSW weld for AA6082 and AA5456 plates.	Optimized conditions: traverse speed 200 mm/min, tool rotation 1000 rpm, tool tilt angle 1°, and depth of pin 4 mm. A straight pin profile was the best.	[113]
11	Comparison of underwater FSW and conventional FSW with varying welding speeds.	Conventional FSW at 60 mm/min had maximum strength. Underwater FSW at 45 mm/min yielded the best results.	[114]
12	Dissimilar FSW for A6061 and AA7075 Al alloys with optimized process parameters.	Optimal parameters: 1164 rpm tool rotation, 32 mm/min traverse speed, 8.7% SiC particles. Max tensile strength of 252 MPa and a microhardness of 178 HV.	[115]
13	Effect of plate position on FSW weld characteristics for AA6061 and AA6082.	Better strength with AA6082 on the advancing side. Max tensile strength of 218 MPa along the weldment sample.	[116]
14	Positioning effect on mechanical properties of AA1050-H14 and AA6082-T6 Al alloys.	AA1050-H14 on the advancing side resulted in better mechanical strength. (Tool rotation: 1200 rpm, traverse speed: 40 mm/min, tool tilt: 2°).	[117]
15	Novel heat treatment process effect on grain coarsening for Al2219 alloy.	The intermediate heat treatment process improved weld strength by 20% and reduced crack propagation along the grain boundary.	[118]
16	Welding tubular components using the FSW technique with a novel tool design.	3° concave tool design yielded maximum strength with minimum pores, while higher concavities improved surface roughness.	[119]
17	Joining of AA6061 and AA7075 using FSW with Al_2O_3 reinforcement.	Optimal conditions: 971 rpm tool speed, 40 mm/min traverse speed, and 10% Al_2O_3 volume percentage, resulting in a maximum joint strength of 226.2 MPa and a microhardness of 144.3 HV.	[120]
18	Corrosion behavior of FSW-welded Al6061-T6/AZ31 dissimilar alloy.	Maximum corrosion for sample A1 with the lowest pH value of 2. Increasing welding speed led to a decreased corrosion rate. Impact strength is reduced with decreasing temperature.	[121]
19	Formability for FSW for a dissimilar material of AA6061 and AA2017.	Optimized conditions: 1300 rpm tool rotation, 20 mm/min traverse speed, and 1° tool tilt angle. These conditions provided the best joint in comparison with other conditions.	[122]
20	Impact of the curvature radius of the tool on weld performance.	A curvature radius of less than 7 mm resulted in an accumulation of welding material. A 7 mm curvature radius was critical, with values below it leading to poor joint performance and values above it improving strength.	[123]
21	Effect of pin eccentricity on weld joint for AA5754-H111 and AA6101-T6 alloy.	Optimized conditions: 900 rpm tool rotational speed, 40 mm/min traverse speed, and 0.35 mm pin eccentricity for the FSW of dissimilar alloys.	[124]

FSW (flexural welding) is gaining popularity due to its strength, corrosion resistance, and design freedom. It can join dissimilar materials such EN AW6082 T6 alloy, AA1050 Al alloy, and AZ31 alloy. Researchers have developed new techniques for cooling FSW beads, such as indirect cooling (ICFSW) and optimized operating conditions for various materials. Multi-pass roll and annealing have improved the mechanical properties of welded joints and heat treatment processes have been explored for grain coarsening in the Al2219 alloy.

4.3. Use of Machine Learning and Artificial Intelligence (AI) in Friction Stir Welding

FSW, a solid-state welding and material processing method, is being optimized and increased through simulation and machine learning. This process is used in the aerospace, automotive, and materials research industries. Machine learning helps researchers analyze large data volumes, adjust process parameters, and predict outcomes. Simulation models enable virtual testing, reducing the need for expensive physical trials. This leads to faster development for better FSW processes, improved material characteristics, and lower manufacturing costs.

One study has utilized machine learning to predict the mechanical strength of a FSW weld joint using the dissimilar alloys AA5083 and AA5061. It considered 11 input process parameters and used Gaussian process regression and support vector machine models. The model was found to be more accurate than the other suggested models [125]. A similar study used the decision tree, random forest, and XGBoost models to predict the mechanical properties of the AA6061-T6 alloy. Among all the tested models, the XGBoost model gave an accuracy of more than 95% [126]. Over the past decade, machine learning has been utilized for predicting FSW in various fields, including joint strength prediction, tool failure analysis, and optimizing the processing conditions [127]. In one of the studies, a hybrid approach was used by blending the three different techniques of SVM, relevance vector machine (RVM), and least square SVM. The predicted R^2 value suggested a hybrid approach using the least square SVM-RVM model gave the highest accuracy in predicting the mechanical strength and hardness as response variables [128].

One study tried to form a relationship model using a machine learning approach for FSW weld characteristics and tool condition monitoring (TCM). To predict the tool condition vibrational data, the machining condition was taken as an input using an accelerometer. The study also observed the light-gradient-boosted machine classifier (LGBMC) model worked better than the other tested ML models [129]. A similar study proposed an improved XGBoost classifier algorithm for the prediction of processing conditions leading to a low void formation in the weld zone. The proposed hybrid model gave 90% accuracy in predicting the voids in the FSW process in comparison with other models [130]. The solidification of the FSW process causes various problems with weld strength. One study predicted the ultimate tensile strength of the AA2050 alloy by first optimizing the FSW welding process parameters using ANOVA and response surface approach regression models. To forecast the outcome, the same DOE model was utilized to generate an ML-based model. According to the study's findings, the K-Fold cross-validation method delivered the highest accuracy compared with other ML models [131].

Similarly, the support vector regression model (SVR) was found to be the best ML model for estimating the FS-welded sample's ultimate tensile strength (UTS) and extension/elongation. Furthermore, SVR in conjunction with the particle swarm optimization (PSO) technique (SVR-PSO) provided the fastest convergence in comparison with other metaheuristics model combinations (such as differential evolution (DE) and genetic algorithm (GA)) [132]. A previous study has shown that a data-driven approach can also be used to predict the mechanical behavior of FS-welded AA6061-T6 alloys. The authors employed deep learning approaches, namely long short-term memory (LSTM) and a gated recurrent unit (GRU) for the accurate prediction of mechanical behavior. A GRU deep learning model predicted the properties with more accuracy and showed the fast response [133].

A similar deep learning model, viz. the ensemble deep learning technique, was used by researchers to predict the weld quality by preparing an ML model based on images of the weld seam for different conditions. Five different CNN models were combined to form an ensemble heterogenous model of deep learning. A large data set of 1664 weld seam images were processed to train the deep learning model. The model was tested for AA5083 and AA5061 dissimilar alloy welding. The used model predicted the output with 96% accuracy [134]. The researchers also explored deep learning (DL)-based deep multilayer perceptron (DMLP), an LSTM model for the prediction of an optimized condition of working for mechanical strength. The DMLP model used in the study was observed to be better than the other DL-based techniques, such as the shallow artificial neural network (SANN) and ANFIS models that have a higher error [135].

One study has established a wavelet transformation approach for dissimilar welding characteristics prediction by tracking the force and toque signals when welding Al and Cu dissimilar materials. Different types of signals such as original, approximate, and sum of detail were taken as the bases for processing the values and predicting the output. The study suggested a relationship between the detailed signals and the bead structure and the sum of detail signals and weld microstructure [136].

A similar study used the DNN approach by employing recurrent neural network (RNN), CNN, and RWTH cluster models to predict the weld defect. The study observed that the bidirectional LSTM model had an accuracy greater than 95% for weld defects bigger than 0.08 mm when used for a single type of material and thickness of the Al alloy. Additionally, when the classification model was employed on multi-materials, the accuracy dropped to below 90% [137]. One group of authors explored the backpropagation neural network (BPNN) to predict the strength along with the optimization of FSW processing condition for the Al 2195 alloy. Four-dimensional mapping of output with the processing condition was established with 92% accuracy of the established model. The study suggested a tool rotation of 1810 rpm, a traverse speed of 115 mm/min, and 3 KN of welding pressure as the optimized conditions of FSW processing with a maximum tensile strength of 415 MPa [138]. Similarly, one study developed artificial intelligence (AI)-based models for predicting the mechanical strength of the FSW weld [139]. From the literature, it has been observed that the basic models that have used AI and deep learning have employed the KNN, RNN, LSTM, XGBoost, DMLP, GRU, GA, SVM, etc., models for generating relationships between the process variable and output signal. Table 2 shows the summarized output of the technological advancement in AI and machine learning tools for FSW processing.

Table 2. Summary table for technological advancement in AI and machine learning for FSW.

S. No.	Research Focus	Key Findings	Reference
1	Mechanical strength prediction for AA5083 and AA5061 dissimilar alloys in FSW weld joints	The model used in the study was more accurate than other suggested models.	[125]
2	Mechanical properties prediction for AA6061-T6 alloy	XGBoost model gave an accuracy greater than 95%.	[126]
3	Various applications of machine learning in FSW	The hybrid approach using least square SVM-RVM provided the highest accuracy in predicting mechanical strength and hardness.	[128]
4	Relationship model for FSW weld characteristics and tool condition monitoring (TCM)	LGBMC worked better than other tested ML models.	[129]
5	Prediction of void formation in the FSW process	The hybrid model gave 90% accuracy in predicting voids in the FSW process.	[130]
6	Prediction of ultimate tensile strength for AA2050 alloy	K-Fold cross-validation provided the highest accuracy.	[131]
7	Prediction of ultimate tensile strength and elongation of FS-welded samples	SVR-PSO gave the fastest convergence.	[132]
8	Deep learning for predicting mechanical behavior in AA6061-T6 alloys	GRU deep learning model predicted properties with high accuracy and a fast response.	[133]
9	Prediction of weld quality based on images	The model achieved 96% accuracy for dissimilar alloy welding.	[134]
10	Deep learning for prediction of optimized working conditions for mechanical strength	DMLP model outperformed other deep learning techniques.	[135]
11	Wavelet transformation for dissimilar welding characteristics prediction	Relationship between signal types and output.	[136]
12	Deep learning for predicting weld defects	Bi-directional LSTM achieved accuracy greater than 95% for specific conditions.	[137]
13	Prediction of strength and FSW processing condition for Al 2195 alloy	Established a 92% accurate model for FSW processing conditions.	[138]
14	AI-based models for predicting mechanical strength in FSW welds	Various AI and deep learning models are used for relationship modeling between process variables and output signals.	[139]

FSW, a method for solid-state welding and material processing, is being optimized and increasing in efficiency through simulation and machine learning. Simulation models enable virtual testing and FSW outcome prediction, reducing the need for expensive physical trials. Machine learning has been used for predicting FSW in areas such as joint strength prediction, tool failure analysis, and optimization of processing conditions. A hybrid approach blending SVM, RVM, and least squares SVM was used for high accuracy when predicting mechanical strength and hardness. Deep learning approaches such as long short-term memory (LSTM) and gated recurrent unit (GRU) have been employed for accurate mechanical behavior prediction. A wavelet transformation approach has been developed for dissimilar welding characteristics predictions. DNN approaches, including the recurrent neural network (RNN), CNN, and RWTH cluster models, have been used to predict weld defects and optimize the FSW processing conditions. Artificial intelligence (AI)-based models have also been developed for FSW processing, employing the KNN, RNN, LSTM, XGBoost, DMLP, GRU, GA, and SVM models to generate relationships between the process variables and output signals.

5. Microstructural and Mechanical Characterization

Friction stir welding (FSW) is a solid-state welding process that can cause microstructural and mechanical changes in friction-stir-welded (FSWed) joints. The stirring action refines grains, resulting in microstructural changes that affect the weld's mechanical properties [140]. Mechanical properties such as the hardness, tensile strength, and toughness are affected, making FSW joints suitable for marine applications. Therefore, studying both mechanical and microstructural properties of FSW joints is crucial.

5.1. Microstructural Changes Occurring during FSW

The recrystallization and texture development in the stirred zone during FSW is accredited to the collective effects of intense plastic deformation as well as the high-temperature exposure [141–143]. Similarly, the dissolution of precipitates and their subsequent coarsening are observed within and around the stirred zone [144]. The alterations in microstructure within different zones have a substantial impact on the mechanical properties seen after welding. Consequently, numerous researchers have conducted investigations on the microstructural evolution that occurs during FSW [35,37,145,146]. Three unique zones, namely the stirred (nugget) zone, thermomechanically affected zone (TMAZ), and heat-affected zone (HAZ) [147,148], have been discovered based on the microstructural characterization of grains and precipitates, as depicted in Figure 9 [147], Figure 10a [149] and Figure 10b [150].

FSW produces a refined microstructure in the stirred zone due to intense plastic deformation and frictional heating. The most affected area is the nugget zone, also known as the weld nugget or dynamically recrystallized zone (DXZ). The boundary between the recrystallized nugget zone and the parent metal shows a gradual transition on the tool's moving side and a more distinct demarcation on the tool's moving side [150]. The nugget zone, a part of a material, can be categorized into two types: a basin-shaped nugget, which widens towards its upper surface, and an elliptical nugget, which is elliptical. The morphology of the nugget zone varies based on processing parameters, tool geometry, workpiece temperature, and material thermal conductivity.

The phenomenon of dynamic recrystallization during friction stir welding is widely acknowledged to lead to the formation of fine and equiaxed grains within the nugget zone [151]. The size of the recrystallized grains in FSW materials is significantly influenced by various factors, including the FSW parameters, tool geometry, composition of the workpiece, temperature of the workpiece, vertical pressure, and active cooling. The size of the grains within the weld zone exhibits an upward trend at the upper region of the weld zone, whereas it decreases as one moves away from the centerline of the weld zone.

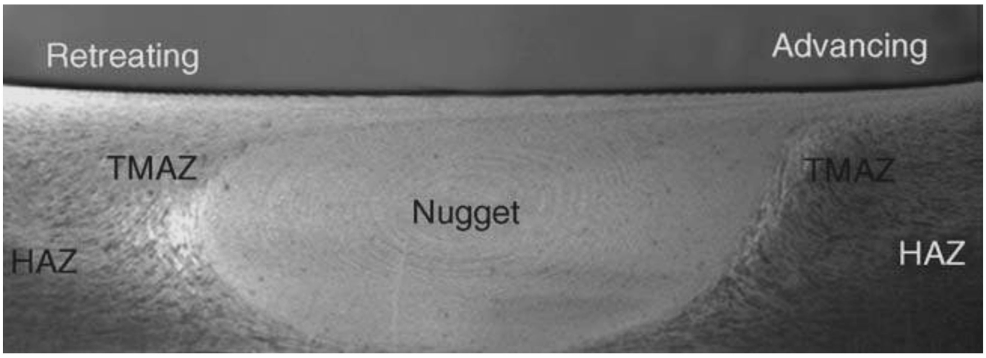

Figure 9. Macrograph showing microstructural zones in the FSW/P of 7075Al-T651 [147].

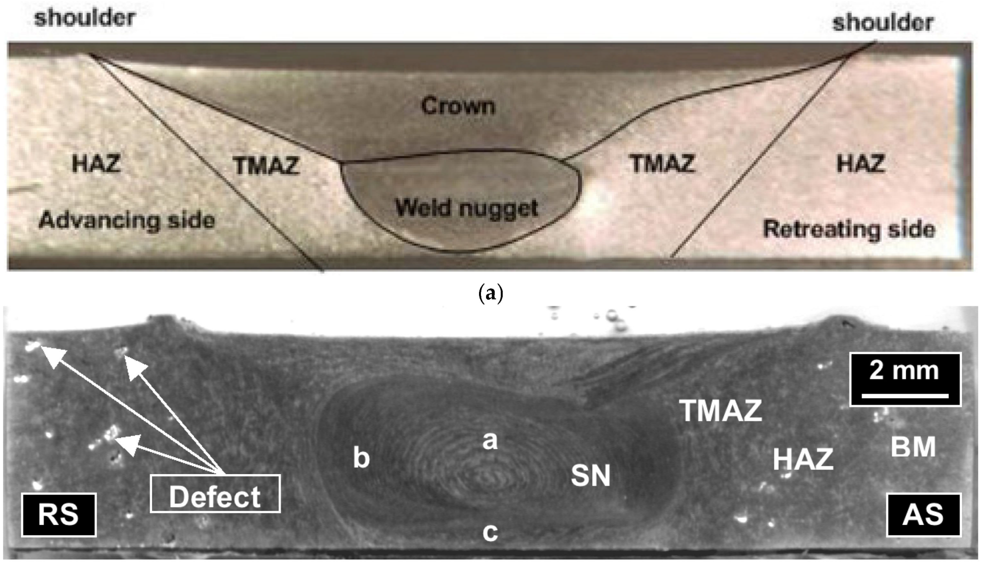

Figure 10. (**a**) Basin-shaped nugget zone [149]; (**b**) elliptical nugget zone [150].

The FSW process is characterized by the formation of a distinct region known as the thermomechanically influenced zone (TMAZ) among the parent substance and the nugget area [152]. During the FSW procedures, the TMAZ is subjected to both heat and mechanical impacts. The TMAZ has a very deformed shape. The parent metal's elongated grains underwent deformation in an upward flow pattern around the nugget zone. The TMAZ is subjected to plastic deformation; however, recrystallization did not occur in this location due to insufficient amounts of deformation strain. Nonetheless, it was discovered that certain precipitates dissolved within the TMAZ as a result of being exposed to high temperatures during the FSW process [153,154]. The degree of disintegration is contingent upon the heat cycle encountered by the TMAZ. Moreover, it has been disclosed that the grains within the TMAZ typically exhibit a notable concentration of sub-boundaries [155]. Figure 11 [156] show a representative TMAZ micrograph.

Figure 11. Schematic of the thermomechanically affected zone (TMAZ) [156].

In addition to the TMAZ, there exists a region known as the heat-affected zone (HAZ). The temperature cycle is observed in this region; however, it does not exhibit any plastic deformation. In their study, Mahoney et al. [157] defined the HAZ, which refers to a region in a heat-treatable aluminum alloy where the temperature exceeds 250°C, resulting in a temperature rise. The HAZ maintains an identical grain structure to that of the parent material. Nevertheless, the precipitate structure is notably impacted by temperature exposures beyond 250 °C. Figure 12 [158] shows the TMAZ micrograph.

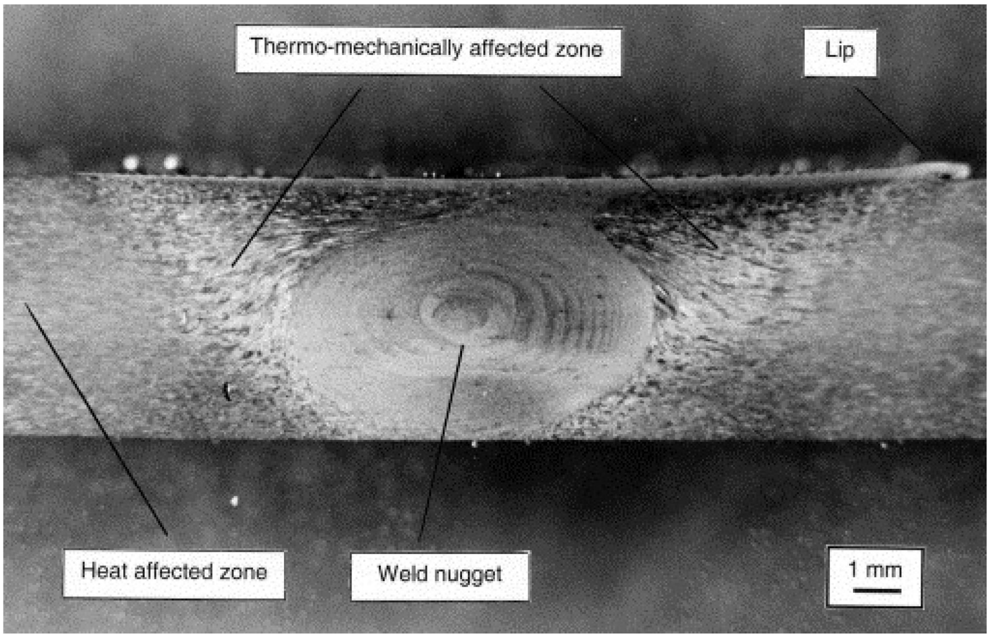

Figure 12. Region of HAZ [158].

5.2. Enhancement in the Mechanical Properties of FSW Joints

Several experiments have provided evidence indicating that the alteration in hardness during friction stir welds varies between precipitation-hardened and solid-solution-hardened aluminum alloys. FSW induces the formation of a thermomechanically affected zone (TMAZ) surrounding the weld center in several precipitation-hardened aluminum alloys [159–161]. Previous studies have proposed that the observed decrease in hardness is a result of the degradation and dissolving of strengthening precipitates that occur throughout the thermal cycle of the friction stir welding process [162–164]. The hardness profiles related to the microstructure in an FSW 6063Al-T5 were investigated by Sato et al. [155]. The researchers observed that the hardness profile in the weld was more significantly influenced by the distribution of precipitates than the size of the grains. A study by Svensson et al. [165] examined the microstructure and characteristics of FSW 5083Al-O. They found that the nugget zone had thin equiaxed grains with a reduced presence of large particles and an increased concentration of small particles. The hardness profile of 5083Al is mainly influenced by dislocation density, as strain hardening is the primary mechanism for its hardening. FSW induced the formation of fine recrystallized grains in the nugget area and recovered/improved grains in the TMAZ of 5083Al-O. Both the nugget area and TMAZ exhibited greater dislocation densities compared with the base material. Both small and large Al6(Mn, Fe) particles were observed in both the nugget zone and the foundation material. The hardness profile in FSW 5083Al could not be well accounted for by the Hall–Petch relationship but was attributed to Orowan strengthening, specifically the overwhelming influence of dispersion strengthening resulting from the distribution of tiny particles.

The solid-state aspect of the FSW technique is widely recognized for its capability to produce joints with exceptional strength, which is a characteristic highly regarded in the field [166]. In contrast to conventional welding techniques, FSW does not depend on the presence of a molten state to form bonds. Conversely, the process involves the utilization of mechanical mixing and forging, leading to the development of a more sophisticated microstructure within the weld. Microstructural refinement is crucial for enhancing joint strength by reducing defects and promoting uniform mechanical properties. The strength of FSW connections is influenced by the base material compatibility, with aluminum alloys showing enhanced strength when subjected to FSW. The ultimate strength of the joint can be influenced by the material's alloy and temper. Post-weld heat treatment (PWHT) can further enhance joint strength by alleviating residual stresses and improving mechanical qualities [167–169].

Achieving a balance between strength and ductility is a complex task in FSW. Although strength is essential in certain situations, it should not be prioritized over ductility. The absence of ductility can lead to brittle characteristics, especially when exposed to dynamic or cyclic loads. Optimizing the process parameters is crucial for achieving this balance [170,171]. Joint ductility is influenced by rotational speed, welding speed, and tool shape, and it is crucial to control these variables to maintain flexibility and optimize strength. Microstructural elements also affect ductility, and FSW can refine joint grain size and texture, thereby enhancing its strength [172,173]. However, it is important to note that this refinement can occasionally have an impact on the ductility of the material. The preservation of ductility necessitates the attainment of an ideal grain structure devoid of any flaws or inclusions.

Fracture toughness is crucial for assessing joint resistance to crack propagation, especially in fatigue-loading situations. The interdependence of strength and ductility in FSW joints requires careful consideration for application. The precise management of process variables, materials, and microstructural elements is necessary to achieve this balance. When implemented effectively, FSW joints can produce strong, ductile joints, ensuring resilient and reliable performance.

5.3. Inclusion of Studies on the Effect of Welding Parameters on the Microstructure and Mechanical Properties

The process of FSW encompasses intricate material displacement and plastic deformation. The material flow pattern and temperature distribution during welding are significantly influenced by the welding settings, tool geometry, and joint design, which in turn affect the microstructural evolution of the material. This section addresses several significant elements that impact the FSW process, including tool geometry, welding settings, and joint design.

The aspect of process development that exerts the most influence is tool geometry [174]. The geometry of the tool is of the utmost importance in determining the flow of material during FSW and subsequently influences the rate at which the welding process can be performed. An FSW tool is composed of a shoulder and a pin, as depicted in Figure 13 [175]. As previously stated, the tool possesses two main functionalities: (a) localized heating and (b) material flow. The tool plunge generates heat due to friction between the pin and workpiece, with additional heating due to material deformation. The tool is inserted until the shoulder contacts the workpiece, with the sizes of the pin and shoulder being crucial. The shoulder region also contains the heated material volume. The instrument's secondary purpose is to agitate and displace it. Tool design governs the microstructure, characteristics, and process loads and typically uses a concave shoulder and threaded cylindrical pins. Other design aspects do not hold the same significance.

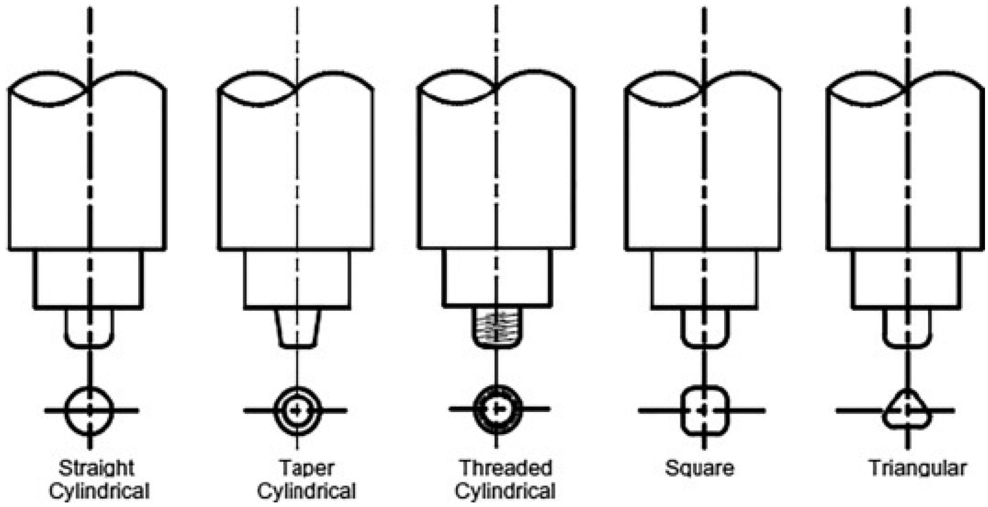

Figure 13. Schematic sketch of the FSW tool and pin profiles [175].

In the context of FSW, two crucial parameters significantly impact the process. These parameters are the tool rotation rate (v, measured in revolutions per minute) and the tool traverse speed (n, measured in millimeters per minute) along the line of the joint [176,177]. The rotational movement of the tool facilitates the stirring and mixing of the material surrounding the spinning pin. The translational movement of a tool transports the stirred material from the front to the back of the pin, completing the welding process. Elevated tool rotation rates lead to increased temperatures due to frictional heating, resulting in enhanced agitation and material blending [178]. The heating process is primarily influenced by the frictional interaction between the tool surface and the workpiece. It is not expected that there will be a monotonic increase in heating as the tool rotation rate increases due to the changing coefficient of friction at the interface. The inclination angle of the spindle or tool about the workpiece's surface is a significant process parameter [179,180].

The insertion depth of a pin into a workpiece is crucial for achieving high-quality welds with seamless tool shoulders. The inclination of the spindle in the trailing direction ensures that the tool's shoulder securely grips the agitated material using a threaded pin, facilitating effective movement. The target depth of the pin also plays a role in achieving seamless tool shoulders. Insufficient depth can result in welds with internal channels or surface grooves. Excessive flash is generated in the workpiece when the tool's shoulder penetrates too deeply during the insertion process, resulting in a concave shape and localized thinning in the welded plates. The latest advancement in tool shoulder design, known as the "scrolled" tool shoulder, allows FSW to be performed with a 08-degree tool tilt, making it ideal for joints with curved surfaces.

6. Corrosion Mitigation and Surface Protection

FSW leads to the formation of different microstructural regions, including the nugget zone, the thermomechanically affected zone (TMAZ), and the heat-affected zone (HAZ). The aforementioned regions demonstrate distinct microstructural attributes, including variations in the residual stress, size of grains, texture, and dislocation density, as well as precipitate size and distribution. Consequently, it is anticipated that the diverse microstructural zones will manifest distinct levels of vulnerability to corrosion [181]. In recent years, several research studies have been undertaken to investigate the impact of FSW on corrosion and stress corrosion cracking (SCC) [182–184].

The initial investigation of pitting and stress corrosion cracking behaviors of FSW 5454Al, as well as the comparison with base alloy and GTAW samples, was conducted by Frankel and Xia [185]. The investigation revealed that pits in FSW samples were generated within the heat-affected zone, whereas in GTAW samples they formed within the extensive dendritic region. FSW welds had superior pitting resistance compared with base alloy and

GTAW welds. The trend of higher pitting potential persisted despite small changes in the pitting potential.

Researchers have also reported that the pitting and SCC resistances of friction-stir-welded (FSW) joints were either superior or equivalent to those of the parent material, based on their experimental observations [186]. Corral et al.'s [182] study examined the impact of friction stir welding (FSW) on the corrosion characteristics of 2024Al-T4 and 2195Al aluminum alloys. They found that FSW joints' diffusion-limited current densities and corrosion potentials were nearly identical to their base alloys when exposed to a 0.6 M sodium chloride solution. Static immersion tests showed comparable by-product accumulation. In a similar vein, Zucchi et al. [183] discovered that the 5083Al FSW weld showed improved corrosion resistance in an EXCO solution of 4 M NaCl, 0.5 M KNO_3, and 0.1 M HNO_3, as well as a lower proclivity for pitting when compared with the base alloy. Furthermore, the FSW weld had a larger pitting potential and a smaller cathodic current than the base alloy. Furthermore, the FSW joint displayed resistance to stress corrosion cracking (SCC) in both environments: EXCO and a solution comprising 3.5% NaCl and 0.3 g/L H_2O_2. MIG joints, on the other hand, were shown to be susceptible to SCC in both solutions.

Multiple investigations have also demonstrated that the pitting capacity of the corrosion area is not only considerably lower than that of the base metal alloy but also lower than that of the nugget area in all friction-stir-welded aluminum joints. The findings of these investigations have demonstrated that the locations with the highest temperatures within the heat-affected zone (HAZ) exhibit the most vulnerability to intergranular corrosion and possess the lowest resistance to pitting, with the nugget being the subsequent region in terms of susceptibility. Microstructural analyses conducted on the regions with the highest temperatures within the heat-affected zone (HAZ) disclosed notable copper (Cu) depletion occurring at the interfaces between grains.

The corrosion mechanism of the intergranular section was attributed to a Cu depletion model by Lumsden et al. [187] based on their experimental data. This model establishes a connection between intergranular corrosion and pitting corrosion. This observation aligns with prior research findings that indicate that the pitting potential exhibits a decline when the concentration of Cu is reduced [188]. In addition, it has been suggested that the preferential corrosion observed in the heat-affected zone (HAZ) can be attributed to the presence of wider partially fused zones (PFZs) and larger grain boundary phases, as well as coarse intragranular precipitates. It is important to note that, apart from alloy chemistry, the residual microstructure present in friction-stir-welded (FSW) joints and the corrosive environment also have a substantial role in influencing the corrosion characteristics of aluminum alloys subjected to FSW.

The potential for the moisture absorption of materials [189] and corrosion in high-strength aluminum friction stir welds is a matter of concern in various engineering applications involving friction stir welding. Several post-weld treatments have been assessed to enhance the corrosion resistance of FSW welds [190]. The impact of the post-weld surface laser treatment on the corrosion resistance of friction-stir-welded (FSW) aluminum welds was examined by Williams et al. [190]. The corrosion tests [191] and electrochemical investigations conducted demonstrated that the excimer laser treatment resulted in a significant enhancement of the resistance to corrosion in FSW welds in 2024Al-T351 alloy as well as 7010Al-T651. The application of a torch treatment involving the exposure of both sides of the friction stir weld (FSW) to a torch flame for 1 min at a distance of 20 mm, followed by water quenching, led to a noticeable reduction in the presence of intragranular precipitates and a general decrease in the occurrence of grain boundary phases [192]. This treatment, particularly effective in the heat-affected zone (HAZ), resulted in a decrease in susceptibility to intergranular corrosion and an enhancement in resistance to stress corrosion cracking [193]. Figure 14 illustrates a standard stress–strain diagram [187] that indicates the mechanical behavior for both naturally and artificially aged friction-stir-welded (FSW) joints that were subjected to testing at a strain rate of 10^{-6} s^{-1} in a 3.5% sodium chloride (NaCl) solution.

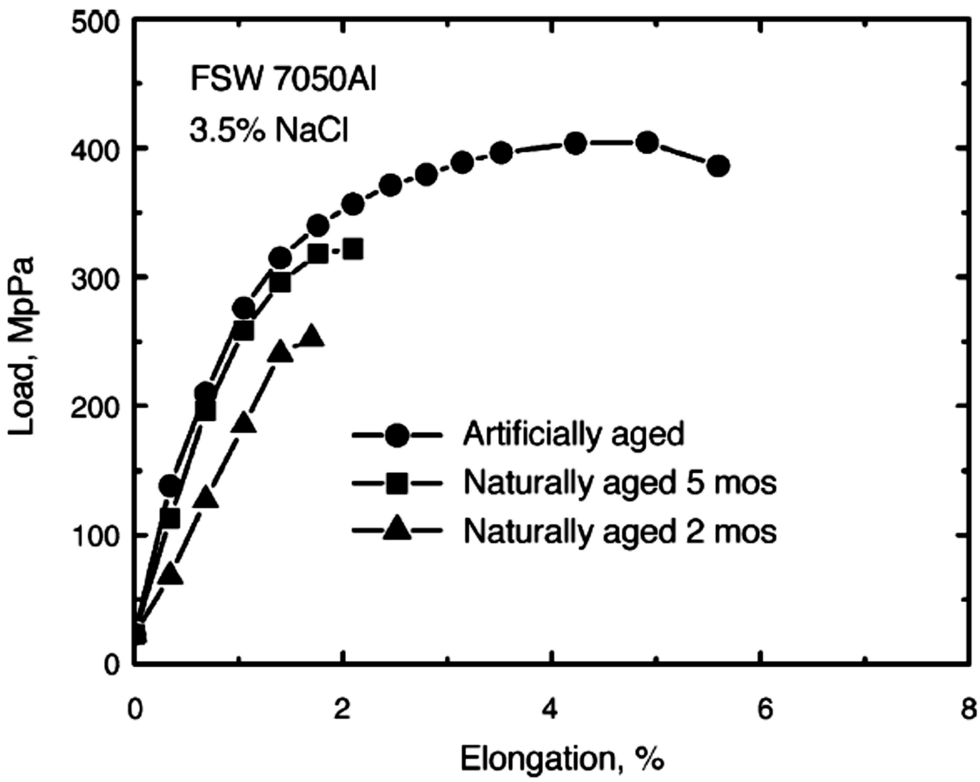

Figure 14. The stress–strain behavior of aged FSW AA7050Al-T7651 specimens (by natural and artificial methods) were examined under a slow strain rate of 1×10^{6} s^{-1} in a 3.5% NaCl solution, as reported by Lumsden et al. [187].

An artificial aging procedure at 100 °C for one week resulted in a significant improvement in the material's resistance to SCC. Additional studies on artificial aging treatments have also been conducted and the restoration of SCC resistance has been proven. However, when subjected to typical environmental conditions, these treatments resulted in an undesirable loss in mechanical properties. A specific heat treatment, consisting of a stabilization heat treatment followed by retrogression and re-aging, was also discovered to have the greatest potential for regaining resistance to stress corrosion cracking (SSC).

7. Future Trends of FSW

FSW (friction stir welding) is a welding technique that enhances the strength and mechanical properties by preventing melting and solidification. It is ideal for marine engineering, especially in combining dissimilar materials such as aluminum alloys due to their corrosion resistance and minimal cleanup after welding. FSW is expanding to include high-strength steels, titanium alloys, and composites, making vessels stronger, lighter, and more resistant to corrosion. When combined with laser welding, hybrid FSW opens up new possibilities for joining different materials for creative uses such as hybrid hull designs, allowing FSW to tailor the vessel properties to meet specific requirements [194–198].

Real-time welding parameter monitoring and analysis using FSW and data analytics can optimize the weld quality and minimize flaws. Laser-aided friction stir welding (LAFSW), a hybrid technique, improves welded junction characteristics by preheating the workpiece and reducing the tool wear and plunging force. This technique allows for material joining and improved control over the welding process. LAFSW has shown promising results in fields such as the aerospace, marine, and automotive industries, where strong welds are crucial for structural integrity and performance. FSAW enhances the mechanical and microstructural properties of joints [199,200].

FSW is expanding its material capabilities to include composites, titanium alloys, high-strength steels, and aluminum alloys to create stronger, lighter, and corrosion-resistant vessels for saltwater settings. A combination of laser welding and FSW will enable hybrid hull designs, encouraging innovation in shipbuilding. FSW will also customize the vessel's properties by incorporating various materials, such as titanium alloys for weight reduction and composite materials for corrosion resistance [201].

Technological integration will optimize the welding process by integrating it with automation technologies, including advanced robots, allowing for real-time monitoring and analysis to maximize weld quality and reduce defects. Innovative methods such as laser-aided friction stir welding (LAFSW) [202] and friction stir additive manufacturing (FSAW) [203] will be used to improve the weld characteristics and control over the welding process. LAFSW minimizes the tool wear and force needs while improving the characteristics of welded junctions, making it useful in the aerospace, marine, and automotive industries. FSAW combines the advantages of friction stir welding and additive manufacturing, allowing for complicated shapes with increased durability and strength.

8. Concluding Remarks and Future Studies

FSW is an efficient process for joining materials, particularly in marine applications such as underwater joints. This study reviews recent developments in FSW and its marine applications, exploring the factors and parameters that affect its significance in the marine industries. It provides a simple solution for joining metals with each other. FSW's fundamental principle and workings have been thoroughly discussed, with a focus on FSW's ability to create high-strength joints with enhanced mechanical and corrosion properties.

→ The study investigates the influence of FSW parameters on material microstructural changes, revealing that tool stirring, grain refining, and super plasticity enhance the joint mechanical properties, enhancing the efficiency and economic feasibility in marine applications. It emphasizes the need for materials compatible with FSW to withstand harsh marine conditions and reduce corrosion.

→ This paper explores future research in FSW for maritime engineering, highlighting the need to integrate environmental and economic factors for sustainability and cost efficiency in large-scale marine endeavors. The maritime sector should develop methodologies that enhance efficiency and productivity while mitigating its ecological impact. The paper highlights the significant contribution of FSW to these objectives and encourages its full utilization.

→ The study highlights the significant impact of FSW in marine applications, highlighting its ability to improve joint strength, corrosion resistance, and fatigue performance. It emphasizes the importance of choosing materials compatible with FSW for project sustainability.

→ The study examines the welding processes' microstructural and mechanical aspects, emphasizing parameter optimization. It contributes to marine structure preservation by minimizing corrosion and protecting surfaces. Future research should focus on advanced FSW apparatus, novel materials, and environmental impact mitigation strategies.

FSW technology is revolutionizing the maritime industry by improving the efficiency and longevity of marine structures while aligning with environmental and economic goals. Its potential to propel the sector towards enhanced efficiency, resilience, and environmental responsibility is evident through ongoing research, innovative approaches, and a commitment to sustainable practices. Despite being in its early stages, FSW's potential for advancement and development in marine applications presents significant implications for the future of the marine sector.

Author Contributions: Conceptualization, investigation, data curation, and writing—original draft were performed by S.B. and S.K., validation, visualization, methodology, formal analysis, and revision/review/editing—original draft were performed by S.B., S.K., I.S., D.K., S.S.B., M.R.A. and S.S.R.K.; supervision, project administration, resources, and funding acquisition was performed by S.K. and S.S.R.K. All authors have read and agreed to the published version of the manuscript.

Funding: The research was financially supported by Universität der Bundeswehr München and the authors would like to acknowledge the support from Universiti Teknologi Malaysia for the funding under UTM R&D (R.J130000.77514J509). Also, the authors are highly thankful to the DY Patil International University, Akurdi, Pune, Maharashtra, India, and CT University Ludhiana, Punjab, India for providing continuous moral and technical support.

Institutional Review Board Statement: Not applicable.

Informed Consent Statement: Not applicable.

Data Availability Statement: Data will be made available on request.

Acknowledgments: The authors are highly thankful to the DY Patil International University, Akurdi, Pune, Maharashtra, India, and CT University Ludhiana, Punjab, India for providing continuous moral and technical support. Also, the authors would like to acknowledge the support from Universiti Teknologi Malaysia for the funding under UTM R&D (R.J130000.77514J509), and the financial support by Universität der Bundeswehr München.

Conflicts of Interest: The authors have no relevant financial or non-financial interests to disclose.

References

1. Singh, S.; Kumar, V.; Kumar, S.; Kumar, A. Variant of MIG welding of similar and dissimilar metals: A review. *Mater. Today Proc.* **2022**, *56*, 3550–3555. [CrossRef]
2. Fande, A.W.; Taiwade, R.V.; Raut, L. Development of activated tungsten inert gas welding and its current status: A review. *Mater. Manuf. Process.* **2022**, *37*, 841–876. [CrossRef]
3. Arora, H.; Singh, R.; Brar, G.S. Thermal and structural modelling of arc welding processes: A literature review. *Meas. Control.* **2019**, *52*, 955–969. [CrossRef]
4. Singh, R.P.; Kumar, S.; Dubey, S.; Singh, A. A review on working and applications of oxy-acetylene gas welding. *Mater. Today Proc.* **2021**, *38*, 34–39. [CrossRef]
5. Acherjee, B. Hybrid laser arc welding: State-of-art review. *Opt. Laser Technol.* **2018**, *99*, 60–71. [CrossRef]
6. Sambasivam, S.; Gupta, N.; Jassim, A.S.; Singh, D.P.; Kumar, S.; Giri, J.M.; Gupta, M. A review paper of FSW on dissimilar materials using aluminum. *Mater. Today Proc.* **2023**. [CrossRef]
7. Akbari, M.; Asadi, P.; Sadowski, T. A Review on Friction Stir Welding/Processing: Numerical Modeling. *Materials* **2023**, *16*, 5890. [CrossRef]
8. ShivaKumar, G.N.; Rajamurugan, G. Friction stir welding of dissimilar alloy combinations—A Review. *Proc. Inst. Mech. Engineers. Part C J. Mech. Eng. Sci.* **2022**, *236*, 6688–6705. [CrossRef]
9. Gebreamlak, G.; Palani, S.; Sirhabizu, B.; Atnaw, S.M.; Gebremichael, E. Dissimilar friction stir welding process—A review. *Adv. Mater. Process. Technol.* **2022**, *8*, 3900–3922. [CrossRef]
10. Singh, V.; Kumar, R.; Kumar, A.; Dewangan, A.K. Automotive light weight multi-materials sheets joining through friction stir welding technique: An overview. *Mater. Today Proc.* **2023**. [CrossRef]
11. Thomas, W.; Nicholas, E.; Needham, J.; Murch, M. Improvements Relating to Friction Welding. WO1993010935A1, 8 November 1995. Available online: https://patents.google.com/patent/WO1993010935A1/enIt.pdf (accessed on 30 October 2023).
12. Singh, V.P.; Patel, S.K.; Kumar, N.; Kuriachen, B. Parametric effect on dissimilar friction stir welded steel-magnesium alloys joints: A review. *Science Technol. Weld. Join.* **2019**, *24*, 653–684. [CrossRef]
13. Threadgilll, P.L.; Leonard, A.J.; Shercliff, H.R.; Withers, P.J. Friction stir welding of aluminum alloys. *Int. Mater. Rev.* **2009**, *54*, 49–93. [CrossRef]
14. Ahmed, S.; Rahman, R.A.U.; Awan, A.; Ahmad, S.; Akram, W.; Amjad, M.; Yahya, M.Y.; Koloor, S.S.R. Optimization of Process Parameters in Friction Stir Welding of Aluminum 5451 in Marine Applications. *J. Mar. Sci. Eng.* **2022**, *10*, 1539. [CrossRef]
15. Di Bella, G.; Alderucci, T.; Favaloro, F.; Borsellino, C. Effect of tool tilt angle on mechanical resistance of AA6082/AA5083 friction stir welded joints for marine applications. *Procedia CIRP* **2023**, *118*, 879–884. [CrossRef]
16. Gibson, B.; Lammlein, D.; Prater, T.; Longhurst, W.; Cox, C.; Ballun, M.; Dharmaraj, K.; Cook, G.; Strauss, A. Friction stir welding: Process, automation, and control. *J. Manuf. Process.* **2014**, *16*, 56–73. [CrossRef]
17. Venugopal, V.; Singh, V.P.; Kuriachen, B. Underwater friction stir welding of marine grade aluminium alloys: A review. *Mater. Today Proc.* **2023**. [CrossRef]

18. Di Bella, G.; Alderucci, T.; Salmeri, F.; Cucinotta, F. Integrating the sustainability aspects into the risk analysis for the manufacturing of dissimilar aluminium/steel friction stir welded single lap joints used in marine applications through a Life Cycle Assessment. *Sustain. Futur.* **2022**, *4*, 100101. [CrossRef]
19. Delzendehrooy, F.; Akhavan-Safar, A.; Barbosa, A.; Beygi, R.; Cardoso, D.; Carbas, R.; Marques, E.; da Silva, L. A comprehensive review on structural joining techniques in the marine industry. *Compos. Struct.* **2022**, *289*, 115490. [CrossRef]
20. Kavathia, K.; Badheka, V. Application of FSW in Automotive and Electric Vehicle. *Lect. Notes Intell. Transp. Infrastruct. Part F* **2022**, *1361*, 289–304.
21. Chen, Y.; Nakata, K. Effect of tool geometry on microstructure and mechanical properties of friction stir lap welded magnesium alloy and steel. *Mater. Des.* **2009**, *30*, 3913–3919. [CrossRef]
22. Qiu, R.; Iwamoto, C.; Satonaka, S. The influence of reaction layer on the strength of aluminum/steel joint welded by resistance spot welding. *Mater. Charact.* **2009**, *60*, 156–159. [CrossRef]
23. Chadha, U.; Selvaraj, S.K.; Gunreddy, N.; Babu, S.S.; Mishra, S.; Padala, D.; Shashank, M.; Mathew, R.M.; Kishore, S.R.; Panigrahi, S.; et al. A Survey of Machine Learning in Friction Stir Welding, including Unresolved Issues and Future Research Directions. *Mater. Des. Process. Commun.* **2022**, *2022*, 1–28. [CrossRef]
24. Balachandar, K.; Jegadeeshwaran, R. Friction stir welding tool condition monitoring using vibration signals and Random forest algorithm—A Machine learning approach. *Mater. Today Proc.* **2021**, *46*, 1174–1180. [CrossRef]
25. Nguyen-Le, D.H.; Tao, Q.; Nguyen, V.-H.; Abdel-Wahab, M.; Nguyen-Xuan, H. A data-driven approach based on long short-term memory and hidden Markov model for crack propagation prediction. *Eng. Fract. Mech.* **2020**, *235*, 107085. [CrossRef]
26. Ho, L.V.; Trinh, T.T.; De Roeck, G.; Bui-Tien, T.; Nguyen-Ngoc, L.; Wahab, M.A. An efficient stochastic-based coupled model for damage identification in plate structures. *Eng. Fail. Anal.* **2022**, *131*, 105866. [CrossRef]
27. Elsheikh, A. Bistable Morphing Composites for Energy-Harvesting Applications. *Polymers* **2022**, *14*, 1893. [CrossRef]
28. Najjar, I.; Sadoun, A.; Elaziz, M.A.; Abdallah, A.; Fathy, A.; Elsheikh, A.H. Predicting kerf quality characteristics in laser cutting of basalt fibers reinforced polymer composites using neural network and chimp optimization. *Alex. Eng. J.* **2022**, *61*, 11005–11018. [CrossRef]
29. Wang, S.; Wang, H.; Zhou, Y.; Liu, J.; Dai, P.; Du, X.; Wahab, M.A. Automatic laser profile recognition and fast tracking for structured light measurement using deep learning and template matching. *Measurement* **2021**, *169*, 108362. [CrossRef]
30. Elsheikh, A.H. Applications of machine learning in friction stir welding: Prediction of joint properties, real-time control and tool failure diagnosis. *Eng. Appl. Artif. Intell.* **2023**, *121*, 105961. [CrossRef]
31. Khoshaim, A.B.; Moustafa, E.B.; Bafakeeh, O.T.; Elsheikh, A.H. An Optimized Multilayer Perceptrons Model Using Grey Wolf Optimizer to Predict Mechanical and Microstructural Properties of Friction Stir Processed Aluminum Alloy Reinforced by Nanoparticles. *Coatings* **2021**, *11*, 1476. [CrossRef]
32. Shokri, V.; Sadeghi, A.; Sadeghi, M. Thermomechanical modeling of friction stir welding in a Cu-DSS dissimilar joint. *J. Manuf. Process.* **2018**, *31*, 46–55. [CrossRef]
33. Çam, G.; Javaheri, V.; Heidarzadeh, A. Advances in FSW and FSSW of dissimilar Al-alloy plates. *J. Adhes. Sci. Technol.* **2023**, *37*, 162–194. [CrossRef]
34. Singh, R.P.; Dubey, S.; Singh, A.; Kumar, S. A review paper on friction stir welding process. *Mater. Today Proc.* **2021**, *38*, 6–11. [CrossRef]
35. Rudrapati, R. Effects of welding process conditions on friction stir welding of polymer composites: A review. *Compos. Part C Open Access* **2022**, *8*, 100269. [CrossRef]
36. Uday, K.N.; Rajamurugan, G. Influence of process parameters and its effects on friction stir welding of dissimilar aluminium alloy and its composites—A review. *J. Adhes. Sci. Technol.* **2023**, *37*, 767–800. [CrossRef]
37. Ambrosio, D.; Morisada, Y.; Ushioda, K.; Fujii, H. Material flow in friction stir welding: A review. *J. Mater. Process. Technol.* **2023**, *320*, 118116. [CrossRef]
38. Chandana, R.; Saraswathamma, K. Impact of tool pin profiles in friction stir welding process—A review. *Mater. Today Proc.* **2023**, *76*, 602–606. [CrossRef]
39. Mohan, D.G.; Wu, C. A Review on Friction Stir Welding of Steels. *Chin. J. Mech. Eng.* **2021**, *34*, 137. [CrossRef]
40. De Giorgi, M.; Scialpi, A.; Panella, F.W.; De Filippis, L.A.C. Effect of shoulder geometry on residual stress and fatigue properties of AA6082 fsw joints. *J. Mech. Sci. Technol.* **2009**, *23*, 26–35. [CrossRef]
41. Tiwari, A.; Singh, P.; Pankaj, P.; Biswas, P.; Kore, S.D. FSW of low carbon steel using tungsten carbide (WC-10wt.%Co) based tool material. *J. Mech. Sci. Technol.* **2019**, *33*, 4931–4938. [CrossRef]
42. Siddiquee, A.N.; Pandey, S. Experimental investigation on deformation and wear of WC tool during FSW of stainless steel. *Int. J. Adv. Manuf. Technol.* **2014**, *73*, 479–486. [CrossRef]
43. Raj, S.; Pankaj, P.; Biswas, P. Friction Stir Welding of Inconel-718 Alloy Using a Tungsten Carbide Tool. *J. Mater. Eng. Perform.* **2022**, *31*, 2086–2101. [CrossRef]
44. Mystica, A.; Sankavi, S.; Sakthi, V.S.; Ganesh, T.; Kumar, V.S. Heat Reduction in a Tool Holder during Friction Stir Welding of Aluminium Alloy. *Appl. Mech. Mater.* **2015**, *766–767*, 705–711. [CrossRef]
45. Derazkola, H.A.; García, E.; Eyvazian, A.; Aberoumand, M. Effects of Rapid Cooling on Properties of Aluminum-Steel Friction Stir Welded Joint. *Materials* **2021**, *14*, 908. [CrossRef] [PubMed]

46. Emamian, S.; Awang, M.; Yusof, F.; Hussain, P.; Mehrpouya, M.; Kakooei, S.; Moayedfar, M.; Zafar, A. A Review of Friction Stir Welding Pin Profile. In Proceedings of the 2nd International Conference on Mechanical, Manufacturing and Process Plant Engineering, Kuala Lumpur, Malaysia, 23–24 November 2016; pp. 1–18.
47. Padmanaban, G.; Balasubramanian, V. Selection of FSW tool pin profile, shoulder diameter and material for joining AZ31B magnesium alloy—An experimental approach. *Mater. Des.* **2009**, *30*, 2647–2656. [CrossRef]
48. Ding, R.J.; Oelgoetz, P.A. *Mechanical Property Analysis in the Retracted Pin-Tool (RPT) Region of Friction Stir Welded (FSW) Aluminum Lithium 2195*; NASA: Thousand Oaks, CA, USA, 1999.
49. Chen, G.; Wang, G.; Shi, Q.; Zhao, Y.; Hao, Y.; Zhang, S. Three-dimensional thermal-mechanical analysis of retractable pin tool friction stir welding process. *J. Manuf. Process.* **2019**, *41*, 1–9. [CrossRef]
50. Quintana, K.J.; Silveira, J.L.L. Threaded pin effects analysis on forces in FSW. *J. Braz. Soc. Mech. Sci. Eng.* **2021**, *43*, 491. [CrossRef]
51. Meyghani, B.; Awang, M.B.; Emamian, S.S.; Nor, M.K.B.M.; Pedapati, S.R. A Comparison of Different Finite Element Methods in the Thermal Analysis of FSW. *Metals* **2017**, *7*, 450. [CrossRef]
52. Sillapasa, K.; Mutoh, Y.; Miyashita, Y.; Seo, N. Fatigue Strength Estimation Based on Local Mechanical Properties for Aluminum Alloy FSW Joints. *Materials* **2017**, *10*, 186. [CrossRef]
53. Dudzik, K.; Jurczak, W. Influence of Friction Stir Welding on Corrosion Properties of Aw-7020M Alloy in Sea Water. *Adv. Mater. Sci.* **2015**, *15*, 7–13. [CrossRef]
54. Ramesh, N.; Kumar, V.S. Experimental erosion-corrosion analysis of friction stir welding of AA 5083 and AA 6061 for sub-sea applications. *Appl. Ocean Res.* **2020**, *98*, 102121. [CrossRef]
55. Golubev, I.A.; Chernikov, E.V.; Naumov, A.A.; Michailov, V.G. Temperature distribution and welding distortion measurements after FSW of Al 6082-T6 sheets. In *Friction Stir Welding and Processing VIII*; Springer International Publishing: Cham, Switzerland, 2015; pp. 289–295.
56. Kah, P.; Rajan, R.; Martikainen, J.; Suoranta, R. Investigation of weld defects in friction-stir welding and fusion welding of aluminium alloys. *Int. J. Mech. Mater. Eng.* **2015**, *10*, 26. [CrossRef]
57. Murr, L.E. A Review of FSW Research on Dissimilar Metal and Alloy Systems. *J. Mater. Eng. Perform.* **2010**, *19*, 1071–1089. [CrossRef]
58. Morishige, T.; Kawaguchi, A.; Tsujikawa, M.; Hino, M.; Hirata, T.; Higashi, K. Dissimilar Welding of Al and Mg Alloys by FSW. *Mater. Trans.* **2008**, *49*, 1129–1131. [CrossRef]
59. Karlsson, L.; Berqvist, E.-L.; Larsson, H. Application of Friction Stir Welding to Dissimilar Welding. *Weld. World* **2002**, *46*, 10–14. [CrossRef]
60. DebRoy, T.; Bhadeshia, H.K.D.H. Friction stir welding of dissimilar alloys—A perspective. *Sci. Technol. Weld. Join.* **2010**, *15*, 266–270. [CrossRef]
61. Chien, C.-H.; Lin, W.-B.; Chen, T. Optimal FSW process parameters for aluminum alloys AA5083. *J. Chinese Inst. Eng.* **2011**, *34*, 99–105. [CrossRef]
62. Eslami, N.; Hischer, Y.; Harms, A.; Lauterbach, D.; Böhm, S. Optimization of Process Parameters for Friction Stir Welding of Aluminum and Copper Using the Taguchi Method. *Metals* **2019**, *9*, 63. [CrossRef]
63. Elangovan, K.; Balasubramanian, V.; Valliappan, M. Effect of tool pin profile and tool rotational speed on mechanical properties of friction stir welded AA6061 aluminium alloy. *Mater. Manuf. Process.* **2008**, *23*, 251–260. [CrossRef]
64. Prabha, K.A.; Putha, P.K.; Prasad, B.S. Effect of Tool Rotational Speed on Mechanical Properties of Aluminium Alloy 5083 Weldments in Friction Stir Welding. *Mater. Today Proc.* **2018**, *5*, 18535–18543. [CrossRef]
65. Zhang, Z.; Zhang, H. Numerical studies on the effect of transverse speed in friction stir welding. *Mater. Des.* **2009**, *30*, 900–907. [CrossRef]
66. Liu, F.C.; Hovanski, Y.; Miles, M.P.; Sorensen, C.D.; Nelson, T.W. A review of friction stir welding of steels: Tool, material flow, microstructure, and properties. *J. Mater. Sci. Technol.* **2018**, *34*, 39–57. [CrossRef]
67. Kumar, K.; Kailas, S.V.; Srivatsan, T.S. Influence of Tool Geometry in Friction Stir Welding. *Mater. Manuf. Process.* **2008**, *23*, 188–194. [CrossRef]
68. Arici, A.; Selale, S. Effects of tool tilt angle on tensile strength and fracture locations of friction stir welding of polyethylene. *Sci. Technol. Weld. Join.* **2007**, *12*, 536–539. [CrossRef]
69. Bhukya, S.N.; Wu, Z.; Maniscalco, J.; Elmustafa, A. Effect of copper donor material-assisted friction stir welding of AA6061-T6 alloy on downward force, microstructure, and mechanical properties. *Int. J. Adv. Manuf. Technol.* **2022**, *119*, 2847–2862. [CrossRef]
70. Papahn, H.; Bahemmat, P.; Haghpanahi, M. Effect of cooling media on residual stresses induced by a solid-state welding: Underwater FSW. *Int. J. Adv. Manuf. Technol.* **2016**, *83*, 1003–1012. [CrossRef]
71. Scutelnicu, E.; Birsan, D.; Cojocaru, R. Research on Friction Stir Welding and Tungsten Inert Gas assisted Friction Stir Welding of Copper. Available online: http://www.cmrs.ugal.ro (accessed on 31 October 2023).
72. Bo, L.N.; Cojocaru, R. ISIM Achievements Regarding Friction Stir Welding in Inert Gas Environment. *Adv. Mater. Res.* **2022**, *1172*, 15–24. [CrossRef]
73. Martin, J.; Wei, S. Friction stir welding technology for marine applications. In *Friction Stir Welding and Processing VIII*; Springer International Publishing: Cham, Switzerland, 2015; pp. 219–226.
74. Feistauer, E.; Bergmann, L.; Barreto, L.; dos Santos, J. Mechanical behaviour of dissimilar friction stir welded tailor welded blanks in Al–Mg alloys for Marine applications. *Mater. Des.* **2014**, *59*, 323–332. [CrossRef]

75. Wahid, M.A.; Siddiquee, A.N.; Khan, Z.A. Aluminum alloys in marine construction: Characteristics, application, and problems from a fabrication viewpoint. *Mar. Syst. Ocean Technol.* **2020**, *15*, 70–80. [CrossRef]
76. Shanavas, S.; Dhas, J.E.R. Parametric optimization of friction stir welding parameters of marine grade aluminium alloy using response surface methodology. *Trans. Nonferrous Met. Soc. China* **2017**, *27*, 2334–2344. [CrossRef]
77. Konkol, P.J.; Mathers, J.A.; Johnson, R.; Pickens, J.R. Friction Stir Welding of HSLA-65 Steel for Shipbuilding. *J. Sh. Prod.* **2003**, *19*, 159–164. [CrossRef]
78. Sekban, D.M.; Aktarer, S.M.; Purcek, G. Friction Stir Welding of Low-Carbon Shipbuilding Steel Plates: Microstructure, Mechanical Properties, and Corrosion Behavior. *Metall. Mater. Trans. A* **2019**, *50*, 4127–4140. [CrossRef]
79. Sabry, I.; Mourad, A.-H.I.; Thekkuden, D.T. Comparison of Mechanical Characteristics of Conventional and Underwater Friction Stir Welding of AA 6063 Pipe Joints. *Int. Rev. Mech. Eng.* **2020**, *14*, 64. [CrossRef]
80. Saravanakumar, R.; Rajasekaran, T.; Pandey, C.; Menaka, M. Mechanical and Microstructural Characteristics of Underwater Friction Stir Welded AA5083 Armor-Grade Aluminum Alloy Joints. *J. Mater. Eng. Perform.* **2022**, *31*, 8459–8472. [CrossRef]
81. Sabry, I.; Allah, N.G.; Nour, M.A.; Ghafaar, M.A. Mechanical Characteristic of Al 6063 Pipe Joined by Underwater Friction Stir Welding. In *Proceedings of Fourth International Conference on Inventive Material Science Applications*; Springer: Singapore, 2022; pp. 689–699.
82. Sebok, K.F. Design, Fabrication and Operation of A3000 FSW Submersible Work System. In Proceedings of the Offshore Technology Conference, Houston, TX, USA, 8–10 May 1978. [CrossRef]
83. Polezhayeva, H.; Toumpis, A.I.; Galloway, A.M.; Molter, L.; Ahmad, B.; Fitzpatrick, M.E. Fatigue performance of friction stir welded marine grade steel. *Int. J. Fatigue* **2015**, *81*, 162–170. [CrossRef]
84. Delaune, P.T. On-Site Welded Repairs To Offshore Structures Using Dry Underwater Habitats. In Proceedings of the Offshore Technology Conference, Houston, TX, USA, 8–10 May 1978. [CrossRef]
85. Lader, S.K.; Baruah, M.; Ballav, R. Significance of underwater friction stir welding on the weld integrity of thin sheets of aluminum (AA1050-O) and brass (CuZn34) joints. *Mater. Sci. Eng. A* **2023**, *865*, 144627. [CrossRef]
86. Ahmed, M.M.Z.; Seleman, M.M.E.-S.; Fydrych, D.; Çam, G. Friction Stir Welding of Aluminum in the Aerospace Industry: The Current Progress and State-of-the-Art Review. *Materials* **2023**, *16*, 2971. [CrossRef] [PubMed]
87. Kilic, S.; Ozturk, F.; Demirdogen, M.F. A comprehensive literature review on friction stir welding: Process parameters, joint integrity, and mechanical properties. *J. Eng. Res.* **2023**. [CrossRef]
88. Nathan, S.R.; Balasubramanian, V.; Rao, A.G.; Sonar, T.; Ivanov, M.; Rajendran, C. Influence of tool plunging rate on mechanical properties and microstructure of friction stir welded DMR249A high strength low alloy (HSLA) steel butt joints. *Mater. Test.* **2023**, *65*, 1528–1538. [CrossRef]
89. Osman, M.; Tamin, N. Influence of tool pin profile on the mechanical strength and surface roughness of AA6061-T6 overlap joint friction stir welding. *J. Mech. Eng. Sci.* **2023**, *17*, 9576–9585. [CrossRef]
90. Sundar, A.S.; Kar, A.; Mugada, K.K.; Kumar, A. Enhancement of microstructure, micro-texture, and mechanical properties of Al6061 friction stir welds using the developed static shoulder welding tool. *Mater. Charact.* **2023**, *203*, 113148. [CrossRef]
91. Akbari, M.; Aliha, M.; Berto, F. Investigating the role of different components of friction stir welding tools on the generated heat and strain. *Forces Mech.* **2023**, *10*, 100166. [CrossRef]
92. Arif, M.; Kumar, D.; Siddiquee, A.N. Morphological and Mechanical Characterization of Friction Stir Welded Zones in Acrylonitrile Butadiene Styrene (ABS) Polymer. *J. Mater. Eng. Perform.* **2023**, 1–11. [CrossRef]
93. Hossfeld, M. On Friction, Heat Input, and Material Flow Initiation during Friction Stir Welding: Tool and Process Optimization. *J. Manuf. Mater. Process.* **2023**, *7*, 34. [CrossRef]
94. Mironov, S.Y. Temperature Distribution within the Friction Stir Welding Tool. *Phys. Mesomech.* **2023**, *26*, 33–38. [CrossRef]
95. Shi, L.; Chen, J.; Yang, C.; Chen, G.; Wu, C. Thermal-fluid-structure coupling analysis of void defect in friction stir welding. *Int. J. Mech. Sci.* **2023**, *241*, 107969. [CrossRef]
96. Ahmed, M.M.Z.; Essa, A.R.S.; Ataya, S.; Seleman, M.M.E.-S.; El-Aty, A.A.; Alzahrani, B.; Touileb, K.; Bakkar, A.; Ponnore, J.J.; Mohamed, A.Y.A. Friction Stir Welding of AA5754-H24: Impact of Tool Pin Eccentricity and Welding Speed on Grain Structure, Crystallographic Texture, and Mechanical Properties. *Materials* **2023**, *16*, 2031. [CrossRef]
97. Iftikhar, S.H.; Mourad, A.-H.I.; Thekkuden, D.T.; Cherupurakal, N.; Krishnapriya, R. Friction stir welding of carbon black reinforced high-density polyethylene tube-to-tubesheet joints. *Int. J. Lightweight Mater. Manuf.* **2023**, *6*, 589–605. [CrossRef]
98. Trojovský, P.; Dhasarathan, V.; Boopathi, S. Experimental investigations on cryogenic friction-stir welding of similar ZE42 magnesium alloys. *Alex. Eng. J.* **2023**, *66*, 1–4. [CrossRef]
99. Singh, R.; Kumar, Y. Effect of cooling tank embedded fixture design on the thermal analysis of friction stir welded aluminum alloy. *J. Mater. Eng. Perform.* **2023**, *32*, 7215–7224. [CrossRef]
100. Al-Sabur, R.; Serier, M.; Siddiquee, A.N. Analysis and construction of a pneumatic-powered portable friction stir welding tool for polymer joining. *Adv. Mater. Process. Technol.* **2023**, 1–5. [CrossRef]
101. Senff, M.; Volk, W. Hybrid joining of cast aluminum and steel by compound casting and friction stir welding. *Prod. Eng.* **2023**, *17*, 521–534. [CrossRef]
102. Akbari, M.; Asiabaraki, H.R. Modeling and optimization of tool parameters in friction stir lap joining of aluminum using RSM and NSGA II. *Weld. Int.* **2023**, *37*, 21–33. [CrossRef]

103. Liu, T.S.; Qiu, F.; Yang, H.Y.; Liu, S.; Jiang, Q.C.; Zhang, L.C. Exploring the potential of FSW-ed Al–Zn–Mg–Cu-based composite reinforced by trace in-situ nanoparticles in manufacturing workpiece with customizable size and high mechanical performances. *Compos. Part B Eng.* **2023**, *250*, 110425. [CrossRef]
104. Noga, P.; Skrzekut, T.; Wędrychowicz, M.; Węglowski, M.S.; Węglowska, A. Research of FSW and Electron Beam Welding (EBW) Process for 6082-T6 Aluminum Alloy. *Materials* **2023**, *16*, 4937. [CrossRef] [PubMed]
105. Liu, X.; Ye, T.; Li, Y.; Pei, X.; Sun, Z. Quasi-in-situ characterization of microstructure evolution in friction stir welding of aluminum alloy. *J. Mater. Res. Technol.* **2023**, *25*, 6380–6394. [CrossRef]
106. Singh, R.; Kumar, Y. Microstructural analysis of cooling tank-assisted hybrid friction stir welded aluminium alloys: A novel approach. *Weld. Int.* **2023**, *37*, 445–456. [CrossRef]
107. Kumar, R.; Bhadauria, S.S.; Sharma, V.; Kumar, M. Effect on microstructure and mechanical properties of single pass friction stir welded aluminium alloy AA-7075-T651 joint. *Mater. Today Proc.* **2023**, *80*, 40–47. [CrossRef]
108. Wang, Q.; Zhai, H.; Chen, S.; Wang, L.; Huang, L.; Zhao, J.; Xia, H.; Ma, Y. Simultaneous enhancement of strength and ductility in friction stir welded AZ31 alloy via multi-pass hot-rolling and subsequent annealing. *J. Mater. Res. Technol.* **2023**, *23*, 5181–5192. [CrossRef]
109. Baharudin, B.A.; Mustapha, M.; Ismail, A.; Zulkipli, F.N.; Ayob, F.; Ahmad, A. Microhardness and process parameter optimization of friction stir welding on an AA5052 thin plate. In *Advancements in Materials Science and Technology Led by Women*; Springer: Cham, Switzerland, 2023; pp. 133–141.
110. Kumar, G.V.; Ravishankar, S.S.; Subrahmanyam, M.R.S.; Babu, P.K. An Analysis of Friction Stir Welding of Marine Grade 5083 Aluminium Alloy Using Weld Parameters. *Ind. Eng. J.* **2022**, *51*, 1–7.
111. Vallavi, M.A.; Madhavan, K. Analysing the Influence of Tool Pin on Mechanical Properties of Friction Stir Welded Dissimilar Aluminium Alloys AA6082 & AA5052. *Int. J. Progress. Res. Eng. Manag. Sci.* **2023**. [CrossRef]
112. Laska, A.; Szkodo, M.; Pawłowski, Ł.; Gajowiec, G. Corrosion Properties of Dissimilar AA6082/AA6060 Friction Stir Welded Butt Joints in Different NaCl Concentrations. *Int. J. Precis. Eng. Manuf. Green Technol.* **2023**, *10*, 457–477. [CrossRef]
113. Karumuri, S.; Haldar, B.; Pradeep, A.; Karanam, S.A.K.; Sri, M.N.S.; Anusha, P.; Sateesh, N.; Subbiah, R.; Vijayakumar, S. Multi-objective optimization using Taguchi based grey relational analysis in friction stir welding for dissimilar aluminium alloy. *Int. J. Interact. Des. Manuf.* **2023**. [CrossRef]
114. Datta, R.; Gupta, S.K.; Bhargava, M. Comparison of underwater friction stir welded and conventional friction stir welded AA 5052 alloys based on the mechanical, formability and microstructure behaviour. *Mater. Today Proc.* **2023**. [CrossRef]
115. Jain, S.; Mishra, R.; Mehdi, H.; Gupta, R.; Dubey, A.K. Optimization of processing variables of friction stir welded dissimilar composite joints of AA6061 and AA7075 using response surface methodology. *J. Adhes. Sci. Technol.* **2023**. [CrossRef]
116. Kandasamy, J.; Prakasham, G.; Chaitanya, P.; Eshwar, N. Experimental investigations on the position of plates in friction stir welding of dissimilar alloys. *Mater. Today Proc.* **2023**. [CrossRef]
117. Mabuwa, S.; Msomi, V. The effect of friction stir processing on the friction stir welded AA1050-H14 and AA6082-T6 joints. *Mater. Today Proc.* **2019**, *26*, 193–199. [CrossRef]
118. Wang, Z.; Xu, Y. Effect of a novel intermediate heat treatment process on abnormal grain growth in 2219 aluminum alloy friction stir welds. *Mater. Sci. Eng. A* **2023**, *885*, 145604. [CrossRef]
119. Sen, D.; Pal, S.K.; Panda, S.K. Effect of tool concavity on flash formation during fabrication of tubes through friction stir welding. *Proc. Inst. Mech. Eng. Part B J. Eng. Manuf.* **2023**. [CrossRef]
120. Jain, S.; Mishra, R.S. Multi-response Optimization of Friction Stir Welded Reinforced Joints of Dissimilar Aluminum Alloys. *Trans. Indian Inst. Met.* **2023**. [CrossRef]
121. Singh, V.P.; Kumar, D.; Mahto, R.P.; Kuriachen, B. Microstructural and Mechanical Behavior of Friction-Stir-Welded AA6061-T6 and AZ31 Alloys with Improved Electrochemical Corrosion. *J. Mater. Eng. Perform.* **2023**, *32*, 4185–4204. [CrossRef]
122. Battina, N.M.; Chirala, H.K.; Vanthala, V.S.P.; Javvadi, E.M.; Nukathoti, R.S.; Mohammed, A. Experimental and finite element investigations on formability of friction stir welded tailor welded blanks of AA6061 and AA2017. *Mater. Today Proc.* **2023**. [CrossRef]
123. Qu, L.; Ma, N.; Xiao, X.; Zhang, K.; Li, H. Microstructure and Properties of Nonlinear Lap Joint of 6061 Aluminum Alloy by Friction Stir Welding. *Metals* **2023**, *13*, 1494. [CrossRef]
124. Yogaraj, P.; Kasirajan, L.; Senthamaraikannan, B. Effect of Tool Pin Positioning Factors on the Strength Behavior of Dissimilar Joints of AA5754-H111 and AA6101-T6 by Using Friction Stir Welding. *Trans. Indian Inst. Met.* **2023**, *76*, 3021–3030. [CrossRef]
125. Matitopanum, S.; Pitakaso, R.; Sethanan, K.; Srichok, T.; Chokanat, P. Prediction of the Ultimate Tensile Strength (UTS) of Asymmetric Friction Stir Welding Using Ensemble Machine Learning Methods. *Processes* **2023**, *11*, 391. [CrossRef]
126. Kumar, A.K.; Surya, M.S.; Venkataramaiah, P. Performance evaluation of machine learning based-classifiers in friction stir welding of Aa6061-T6 alloy. *Int. J. Interact. Des. Manuf.* **2023**, *17*, 469–472. [CrossRef]
127. Khaliq, U.A.; Muhamad, M.R.; Yusof, F.; Ibrahim, S.; Isa, M.S.; Chen, Z.; Çam, G. A Review on Friction Stir Butt Welding of Aluminum with Magnesium: A New Insight on Joining Mechanisms by Interfacial Enhancement. *J. Mater. Res. Technol.* **2023**, *27*, 4595–4624. [CrossRef]
128. Ye, X.; Su, Z.; Dahari, M.; Su, Y.; Alsulami, S.H.; Aldhabani, M.S.; Abed, A.M.; Ali, H.E.; Bouzgarrou, S.M. Hybrid modeling of mechanical properties and hardness of aluminum alloy 5083 and C100 Copper with various machine learning algorithms in friction stir welding. *Structures* **2023**, *55*, 1250–1261. [CrossRef]

129. Balachandar, K.; Arockiaraj, K.S.; Sriraman, G.; Jegadeeshwaran, R.; Sakthivel, G.; Lakshmipathi, J. Development of a machine learning model to predict the friction stir welding tool condition. *Mater. Today Proc.* **2023**. [CrossRef]
130. Baruah, A.; Borkar, H. Optimised machine learning classification model to detect void formations in friction stir welding. *Mater. Today Proc.* **2023**. [CrossRef]
131. Anandan, B.; Manikandan, M. Machine learning approach with various regression models for predicting the ultimate tensile strength of the friction stir welded AA 2050-T8 joints by the K-Fold cross-validation method. *Mater. Today Commun.* **2023**, *34*, 105286. [CrossRef]
132. Insua, P.; Nakkiew, W.; Wisittipanich, W. Post Weld Heat Treatment Optimization of Dissimilar Friction Stir Welded AA2024-T3 and AA7075-T651 Using Machine Learning and Metaheuristics. *Materials* **2023**, *16*, 2081. [CrossRef] [PubMed]
133. Dorbane, A.; Harrou, F.; Sun, Y. Exploring Deep Learning Methods to Forecast Mechanical Behavior of FSW Aluminum Sheets. *J. Mater. Eng. Perform.* **2023**, *32*, 4047–4063. [CrossRef]
134. Chiaranai, S.; Pitakaso, R.; Sethanan, K.; Kosacka-Olejnik, M.; Srichok, T.; Chokanat, P. Ensemble Deep Learning Ultimate Tensile Strength Classification Model for Weld Seam of Asymmetric Friction Stir Welding. *Processes* **2023**, *11*, 434. [CrossRef]
135. Modi, U.; Ahmed, S.; Rai, A. Prediction of ultimate tensile strength of friction stir welding joint using deep learning-based-multilayer perceptron and long short term memory networks. *Weld. Int.* **2023**, *37*, 387–399. [CrossRef]
136. Mandal, A.; Banik, A.; Barma, J.D.; Majumdar, G. Friction Stir Welding of Two Dissimilar Metals: Weld Quality Characterization Using the Wavelet Transform Approach. *Iran. J. Sci. Technol. Trans. Mech. Eng.* **2023**. [CrossRef]
137. Rabe, P.; Reisgen, U.; Schiebahn, A. Non-destructive evaluation of the friction stir welding process, generalizing a deep neural defect detection network to identify internal weld defects across different aluminum alloys. *Weld. World* **2023**, *67*, 549–560. [CrossRef]
138. Yu, F.; Zhao, Y.; Lin, Z.; Miao, Y.; Zhao, F.; Xie, Y. Prediction of Mechanical Properties and Optimization of Friction Stir Welded 2195 Aluminum Alloy Based on BP Neural Network. *Metals* **2023**, *13*, 267. [CrossRef]
139. Mishra, A. Artificial intelligence algorithms for prediction of the ultimate tensile strength of the friction stir welded magnesium alloys. *Int. J. Interact. Des. Manuf.* **2023**. [CrossRef]
140. Mishra, R.S.; Mahoney, M.W. *Friction Stir Welding and Processing*; ASM International: Almere, The Netherlands, 2007.
141. Xu, N.; Ueji, R.; Fujii, H. Dynamic and static change of grain size and texture of copper during friction stir welding. *J. Mater. Process. Technol.* **2016**, *232*, 90–99. [CrossRef]
142. Xu, N.; Chen, L.; Feng, R.; Song, Q.; Bao, Y. Recrystallization of Cu-30Zn brass during friction stir welding. *J. Mater. Res. Technol.* **2020**, *9*, 3746–3758. [CrossRef]
143. Heidarzadeh, A.; Mironov, S.; Kaibyshev, R.; Çam, G.; Simar, A.; Gerlich, A.; Khodabakhshi, F.; Mostafaei, A.; Field, D.; Robson, J.; et al. Friction stir welding/processing of metals and alloys: A comprehensive review on microstructural evolution. *Prog. Mater. Sci.* **2021**, *117*, 100752. [CrossRef]
144. Patel, V.; Li, W.; Vairis, A.; Badheka, V. Recent Development in Friction Stir Processing as a Solid-State Grain Refinement Technique: Microstructural Evolution and Property Enhancement. *Crit. Rev. Solid State Mater. Sci.* **2019**, *44*, 378–426. [CrossRef]
145. Salih, O.S.; Ou, H.; Sun, W. Heat generation, plastic deformation and residual stresses in friction stir welding of aluminium alloy. *Int. J. Mech. Sci.* **2023**, *238*, 107827. [CrossRef]
146. Morozova, I.; Królicka, A.; Obrosov, A.; Yang, Y.; Doynov, N.; Weiß, S.; Michailov, V. Precipitation phenomena in impulse friction stir welded 2024 aluminium alloy. *Mater. Sci. Eng. A* **2022**, *852*, 143617. [CrossRef]
147. Mishra, R.S.; Ma, Z.Y. Friction stir welding and processing. *Mater. Sci. Eng. R Rep.* **2005**, *50*, 1–78. [CrossRef]
148. Kumar, K.; Kailas, S.V. The role of friction stir welding tool on material flow and weld formation. *Mater. Sci. Eng. A* **2008**, *485*, 367–374. [CrossRef]
149. Zhang, H.; Khoshnaw, F. Friction stir welding. In *Welding of Metallic Materials. Methods, Metallurgy, and Performance*; Elsevier: Amsterdam, The Netherlands, 2023; pp. 197–228. [CrossRef]
150. Dutta, V.; Kumara, R.; Kumar, V.; Sapkal, V. Influence of FSP on Microstructure and Mechanical Properties of Al Metal Composites (AMCS)—A Review. *J. East China Univ. Sci. Technol.* **2022**, *65*, 555–561. Available online: http://hdlgdxxb.info/index.php/JE_CUST/article/view/131 (accessed on 15 November 2023).
151. Qin, X.; Xu, Y.; Sun, Y.; Fujii, H.; Zhu, Z.; Shek, C.H. Effect of process parameters on microstructure and mechanical properties of friction stir welded CoCrFeNi high entropy alloy. *Mater. Sci. Eng. A* **2020**, *782*, 139277. [CrossRef]
152. Zolghadr, P.; Akbari, M.; Asadi, P. Formation of thermo-mechanically affected zone in friction stir welding. *Mater. Res. Express* **2019**, *6*, 086558. [CrossRef]
153. Jandaghi, M.R.; Pouraliakbar, H.; Hong, S.I.; Pavese, M. Grain boundary transition associated intergranular failure analysis at TMAZ/SZ interface of dissimilar AA7475-AA2198 joints by friction stir welding. *Mater. Lett.* **2020**, *280*, 128557. [CrossRef]
154. Zhang, C.; Huang, G.; Cao, Y.; Zhu, Y.; Huang, X.; Zhou, Y.; Li, Q.; Zeng, Q.; Liu, Q. Microstructure evolution of thermo-mechanically affected zone in dissimilar AA2024/7075 joint produced by friction stir welding. *Vacuum* **2020**, *179*, 109515. [CrossRef]
155. Sato, Y.; Arkom, P.; Kokawa, H.; Nelson, T.; Steel, R. Effect of microstructure on properties of friction stir welded Inconel Alloy 600. *Mater. Sci. Eng. A* **2008**, *477*, 250–258. [CrossRef]
156. El-Sayed, M.M.; Shash, A.; Abd-Rabou, M.; ElSherbiny, M.G. Welding and processing of metallic materials by using friction stir technique: A review. *J. Adv. Join. Process.* **2021**, *3*, 100059. [CrossRef]

157. Mahoney, M.W.; Rhodes, C.G.; Flintoff, J.G.; Bingel, W.H.; Spurling, R.A. Properties of friction-stir-welded 7075 T651 aluminum. *Metall. Mater. Trans. A Phys. Metall. Mater. Sci.* **1998**, *29*, 1955–1964. [CrossRef]
158. Bussu, G.; Irving, P. The role of residual stress and heat affected zone properties on fatigue crack propagation in friction stir welded 2024-T351 aluminium joints. *Int. J. Fatigue* **2003**, *25*, 77–88. [CrossRef]
159. Tao, Y.; Zhang, Z.; Yu, B.; Xue, P.; Ni, D.; Xiao, B.; Ma, Z. Friction stir welding of 2060–T8 AlLi alloy. Part I: Microstructure evolution mechanism and mechanical properties. *Mater. Charact.* **2020**, *168*, 110524. [CrossRef]
160. Ghosh, B.; Das, H.; Samanta, A.; Majumdar, J.D.; Ghosh, M. Majumdar, and M. Ghosh, Influence of tool rotational speed on the evolution of microstructure and mechanical properties of precipitation-hardened Aluminium 6061 butt joint during friction stir welding. *Eng. Res. Express* **2022**, *4*, 015009. [CrossRef]
161. Zeng, X.H.; Xue, P.; Wang, D.; Ni, D.R.; Xiao, B.L.; Ma, Z.Y. Realising equal strength welding to parent metal in precipitation-hardened Al–Mg–Si alloy via low heat input friction stir welding. *Sci. Technol. Weld. Join.* **2018**, *23*, 478–486. [CrossRef]
162. Ni, Y.; Fu, L.; Shen, Z.; Liu, X. Role of tool design on thermal cycling and mechanical properties of a high-speed micro friction stir welded 7075-T6 aluminum alloy. *J. Manuf. Process.* **2019**, *48*, 145–153. [CrossRef]
163. Kalinenko, A.; Vysotskiy, I.; Malopheyev, S.; Mironov, S.; Kaibyshev, R. Influence of the weld thermal cycle on the grain structure of friction-stir joined 6061 aluminum alloy. *Mater. Charact.* **2021**, *178*, 111202. [CrossRef]
164. Wahid, M.A.; Khan, Z.A.; Siddiquee, A.N. Review on underwater friction stir welding: A variant of friction stir welding with great potential of improving joint properties. *Trans. Nonferrous Met. Soc. China* **2018**, *28*, 193–219. [CrossRef]
165. Svensson, L.-E.; Karlsson, L.; Larsson, H.; Karlsson, B.; Fazzini, M.; Karlsson, J. Microstructure and mechanical properties of friction stir welded aluminium alloys with special reference to AA 5083 and AA 6082. *Sci. Technol. Weld. Join.* **2000**, *5*, 285–296. [CrossRef]
166. Eren, B.; Guvenc, M.A.; Mistikoglu, S. Artificial Intelligence Applications for Friction Stir Welding: A Review. *Met. Mater. Int.* **2021**, *27*, 193–219. [CrossRef]
167. Shinde, G.; Gajghate, S.; Dabeer, P.; Seemikeri, C. Low Cost Friction Stir Welding: A Review. *Mater. Today Proc.* **2017**, *4*, 8901–8910. [CrossRef]
168. Wang, G.; Zhao, Y.; Hao, Y. Friction stir welding of high-strength aerospace aluminum alloy and application in rocket tank manufacturing. *J. Mater. Sci. Technol.* **2018**, *34*, 73–91. [CrossRef]
169. Kalinenko, A.; Kim, K.; Vysotskiy, I.; Zuiko, I.; Malopheyev, S.; Mironov, S.; Kaibyshev, R. Microstructure-strength relationship in friction-stir welded 6061-T6 aluminum alloy. *Mater. Sci. Eng. A* **2020**, *793*, 139858. [CrossRef]
170. Zhu, Z.; Sun, Y.; Ng, F.; Goh, M.; Liaw, P.; Fujii, H.; Nguyen, Q.; Xu, Y.; Shek, C.; Nai, S.; et al. Friction-stir welding of a ductile high entropy alloy: Microstructural evolution and weld strength. *Mater. Sci. Eng. A* **2018**, *711*, 524–532. [CrossRef]
171. Lin, P.-T.; Liu, H.-C.; Hsieh, P.-Y.; Wei, C.-Y.; Tsai, C.-W.; Sato, Y.S.; Chen, S.-C.; Yen, H.-W.; Lu, N.-H.; Chen, C.-H. Heterogeneous structure-induced strength-ductility synergy by partial recrystallization during friction stir welding of a high-entropy alloy. *Mater. Des.* **2021**, *197*, 109238. [CrossRef]
172. Wang, Y.; Duan, R.; Hu, J.; Luo, Z.; Ma, Z.; Xie, G. Improvement in toughness and ductility of friction stir welded medium-Mn steel joint via post-welding annealing. *J. Mater. Process. Technol.* **2022**, *306*, 117621. [CrossRef]
173. Khajeh, R.; Jafarian, H.R.; Jabraeili, R.; Eivani, A.R.; Seyedein, S.H.; Park, N.; Heidarzadeh, A. Strength-ductility synergic enhancement in friction stir welded AA2024 alloy and copper joints: Unravelling the role of Zn interlayer's thickness. *J. Mater. Res. Technol.* **2022**, *16*, 251–262. [CrossRef]
174. Kaushik, P.; Dwivedi, D.K. Effect of tool geometry in dissimilar Al-Steel Friction Stir Welding. *J. Manuf. Process.* **2021**, *68*, 198–208. [CrossRef]
175. Khan, N.; Rathee, S.; Srivastava, M. Friction stir welding: An overview on effect of tool variables. *Mater. Today Proc.* **2021**, *47*, 7196–7202. [CrossRef]
176. Wen, Q.; Li, W.; Patel, V.; Gao, Y.; Vairis, A. Investigation on the Effects of Welding Speed on Bobbin Tool Friction Stir Welding of 2219 Aluminum Alloy. *Met. Mater. Int.* **2020**, *26*, 1830–1840. [CrossRef]
177. Amatullah, M.; Jan, M.; Farooq, M.; Zargar, A.S.; Maqbool, A.; Khan, N.Z. Effect of tool rotational speed on the friction stir welded aluminum alloys: A review. *Mater. Today Proc.* **2022**, *62*, 245–250. [CrossRef]
178. Li, Y.; Sun, D.; Gong, W. Effect of Tool Rotational Speed on the Microstructure and Mechanical Properties of Bobbin Tool Friction Stir Welded 6082-T6 Aluminum Alloy. *Metals* **2019**, *9*, 894. [CrossRef]
179. Zhai, M.; Wu, C.; Su, H. Influence of tool tilt angle on heat transfer and material flow in friction stir welding. *J. Manuf. Process.* **2020**, *59*, 98–112. [CrossRef]
180. Rajendran, C.; Srinivasan, K.; Balasubramanian, V.; Balaji, H.; Selvaraj, P. Effect of tool tilt angle on strength and microstructural characteristics of friction stir welded lap joints of AA2014-T6 aluminum alloy. *Trans. Nonferrous Met. Soc. China* **2019**, *29*, 1824–1835. [CrossRef]
181. Xie, Y.; Meng, X.; Wang, F.; Jiang, Y.; Ma, X.; Wan, L.; Huang, Y. Insight on corrosion behavior of friction stir welded AA2219/AA2195 joints in astronautical engineering. *Corros. Sci.* **2021**, *192*, 109800. [CrossRef]
182. Corral, J.; Trillo, E.A.; Li, Y.; Murr, L.E. Corrosion of friction-stir welded aluminum alloys 2024 and 2195. *J. Mater. Sci. Lett.* **2000**, *19*, 2117–2122. [CrossRef]
183. Zucchi, F.; Trabanelli, G.; Grassi, V. Pitting and stress corrosion cracking resistance of friction stir welded AA 5083. *Mater. Corros.* **2001**, *52*, 853–859. [CrossRef]

184. Paglia, C.; Carroll, M.; Pitts, B.; Reynolds, T.; Buchheit, R. Strength, Corrosion and Environmentally Assisted Cracking of a 7075-T6 Friction Stir Weld. *Mater. Sci. Forum* **2002**, *396–402*, 1677–1684. [CrossRef]
185. Frankel, G.S.; Xia, Z. Localized corrosion and stress corrosion cracking resistance of friction stir welded aluminum alloy 5454. *Corrosion* **1999**, *55*, 139–150. [CrossRef]
186. Majumdar, J.D.; Chandra, B.R.; Manna, I. Friction and wear behavior of laser composite surfaced aluminium with silicon carbide. *Wear* **2007**, *262*, 641–648. [CrossRef]
187. Lumsden, J.B.; Mahoney, M.W.; Pollock, G.; Rhodes, C.G. Intergranular corrosion following friction stir welding of aluminum alloy 7075-T651. *Corrosion* **1999**, *55*. [CrossRef]
188. Muller, I.L.; Galvele, J.R. Pitting potential of high purity binary aluminium alloys—II. AlMg and AlZn alloys. *Corros. Sci.* **1977**, *17*, 995–1007. [CrossRef]
189. Wong, K.J.; Johar, M.; Koloor, S.S.R.; Petrů, M.; Tamin, M.N. Moisture absorption effects on mode II delamination of carbon/epoxy composites. *Polymers* **2020**, *12*, 2162. [CrossRef]
190. Williams, S.W.; Ambat, R.; Price, D.; Jariyaboon, M.; Davenport, A.J.; Wescott, A. Laser treatment method for improvement of the corrosion resistance of friction stir welds. *Mater. Sci. Forum* **2003**, *426*, 2855–2860. [CrossRef]
191. Omidi Bidgoli, M.; Reza Kashyzadeh, K.; Rahimian Koloor, S.S.; Petru, M. Estimation of critical dimensions for the crack and pitting corrosion defects in the oil storage tank using finite element method and taguchi approach. *Metals* **2020**, *10*, 1372. [CrossRef]
192. Kim, H.T.; Kil, S.C.; Hwang, W.S.; Cho, W.-S. Investigation on the corrosion behaviour of weld structure. *Corros. Sci. Technol.* **2007**, *6*, 33–35.
193. Khan, M.S.; Abdul-Latif, A.; Koloor, S.S.R.; Petrů, M.; Tamin, M.N. Representative cell analysis for damage-based failure model of polymer hexagonal honeycomb structure under the out-of-plane loadings. *Polymers* **2020**, *13*, 52. [CrossRef] [PubMed]
194. Jacquin, D.; Guillemot, G. A review of microstructural changes occurring during FSW in aluminium alloys and their modelling. *J. Mater. Process. Technol.* **2021**, *288*, 116706. [CrossRef]
195. Sorger, G.; Sarikka, T.; Vilaça, P.; Santos, T.G. Effect of processing temperatures on the properties of a high-strength steel welded by FSW. *Weld. World* **2018**, *62*, 1173–1185. [CrossRef]
196. Gangwar, K.; Ramulu, M. Friction stir welding of titanium alloys: A review. *Mater. Des.* **2018**, *141*, 230–255. [CrossRef]
197. Campanelli, S.L.; Casalino, G.; Casavola, C.; Moramarco, V. Analysis and comparison of friction stir welding and laser assisted friction stir welding of aluminum alloy. *Materials* **2013**, *6*, 5923–5941. [CrossRef] [PubMed]
198. Patil, S.; Nagamadhu, M.; Malyadri, T. A critical review on microstructure and hardness of aluminum alloy 6061 joints obtained by friction stir welding-past, present, and its prospects. *Mater. Today Proc.* **2023**, *82*, 75–78. [CrossRef]
199. Mishra, D.; Gupta, A.; Raj, P.; Kumar, A.; Anwer, S.; Pal, S.K.; Chakravarty, D.; Pal, S.; Chakravarty, T.; Pal, A.; et al. Real time monitoring and control of friction stir welding process using multiple sensors. *CIRP J. Manuf. Sci. Technol.* **2020**, *30*, 1–11. [CrossRef]
200. Vishwakarma, R.P.; Singh, U.K.; Dubey, A.K. Thermal Analysis of Laser-assisted Friction Stir Welding (LAFSW) for Different Geometrical Parameters. *Int. J. Laser Sci. Fundam. Theory Anal. Methods* **2022**, *3*, 65–87.
201. Marode, R.V.; Pedapati, S.R.; Lemma, T.A.; Awang, M. A review on numerical modelling techniques in friction stir processing: Current and future perspective. *Arch. Civ. Mech. Eng.* **2023**, *23*, 154. [CrossRef]
202. Mishra, R.S.; Haridas, R.S.; Agrawal, P. Friction stir-based additive manufacturing. *Sci. Technol. Weld. Join.* **2022**, *27*, 141–165. [CrossRef]
203. Longhurst, W.R.; Strauss, A.M.; E Cook, G.; Cox, C.D.; E Hendricks, C.; Gibson, B.T.; Dawant, Y.S. Investigation of force-controlled friction stir welding for manufacturing and automation. *Proc. Inst. Mech. Eng. Part B J. Eng. Manuf.* **2010**, *224*, 937–949. [CrossRef]